

FINAL TECHNICAL REPORT

**A CRITICAL STUDY OF THE ROLE
OF THE SURFACE OXIDE LAYER
IN TITANIUM BONDING**

by

S. Dias and J. P. Wightman

**Prepared for
National Aeronautics and Space Administration
August, 1983
Grant NAG 1-252**

**NASA-Langley Research Center
Hampton, Virginia 23665
Materials Division
Donald J. Progar**

**Department of Chemistry
Virginia Polytechnic Institute and State University
Blacksburg, Virginia 24061**

FORWARD

This Final Technical Report under NASA Grant NAG 1-252 contains the final draft of the following four manuscripts to be submitted for publication in the Journal of Adhesion:

- 1) Surani S. Dias and J. P. Wightman, "SEM/XPS Analysis of Fractured Adhesively Bonded Ti 6-4 Samples. I. NR 056X".
- 2) Surani S. Dias and J. P. Wightman, "SEM/XPS Analysis of Fractured Adhesively Bonded Ti 6-4 Samples. II. Polyphenylquinoxaline(PPQ)".
- 3) Surani S. Dias and J. P. Wightman, "SEM/XPS Analysis of Fractured Adhesively Bonded Ti 6-4 Samples. III. LARC-13".
- 4) J. A. Skiles, J. Filbey, K. Sanderson and J. P. Wightman, "A Critical Review of the Surface Oxide Layer on Ti-(6Al-4V) Adherends".

SEM/XPS ANALYSIS OF FRACTURED ADHESIVELY BONDED Ti 6-4 SAMPLES.

I. NR 056X

Surani S. Dias and J. P. Wightman
Chemistry Department
Center for Adhesion Science
Polymer Materials and Interfaces Laboratory
Virginia Polytechnic Institute and State University
Blacksburg, VA 24061

A detailed XPS analysis has been made of fractured, thermally aged lap shear samples where the Ti 6-4 adherend was pretreated by both Pasa-Jell etch and chromic acid anodization before bonding with NR 056X polyimide adhesive. Differentiation between cohesive and interfacial failure was based on the absence or presence of a Ti 2p XPS photopeak. The Pasa Jell pretreated Ti 6-4 adherends gave consistently lower lap shear strengths ultimately resulting in interfacial failure after aging 10,000 hrs at 450°F.

INTRODUCTION

There is continuing interest in the development of high temperature structural adhesives (1-3) and in improving the durability of adhesively bonded components (4,5). Recent studies (6) have shown that the properties of the surface oxide layers on Ti 6-4 may play a key role in the understanding of bond durability. The objective of the present research is the SEM/XPS analysis of fractured Ti 6-4 lap shear coupons bonded with NR 056X adhesive and thermally aged for up to 10,000 hours. The lap shear strengths of these samples have been reported (1).

EXPERIMENTAL

Fractured Ti 6-4 lap shear samples were sent from the Boeing Aerospace Company and these panels were used as received. A detailed microscopic/spectroscopic study of similar samples including crack extension measurements has been reported (1,7). The samples used in this study are described in Table I. It is noted that these samples are quite interesting because few bond durability studies (8) have extended to 10,000 hrs at 450°F. The Ti 6-4 adherends were pretreated by both 10V chromic acid anodize and the Pasa-Jell process. The Ti 6-4 panels after pretreatment were bonded with NR 056X. This polyimide is formed by reaction in diglyme of 2,2-bis(3',4'-dicarboxylphenyl) hexa-fluoropropane with a mixture of 4,4'-diaminodiphenyl ether (60%) and p-phenylenediamine (40%). The fractured Ti 6-4 surfaces were categorized as cohesive or interfacial failure based on XPS analysis. A 3/8" diameter sample was punched after visual examination of both fracture surfaces. These punched samples were then assigned to the following groups: metal failure surface (MFS), adhesive failure surface (AFS), metal substrate surface (MSS), and adhesive substrate surface (ASS). A Bausch and Lomb stereo-zoom optical microscope (OM) was used to photograph each punched sample at 20X.

The samples were mounted with copper tape on an aluminum stub. These samples were gold coated and photomicrographs of these specimens were obtained using a JEOL JFM 35c scanning electron microscope.

The XPS studies of the fractured samples were done using a Physical Electronics ESCA/SAM Model 550 electron spectrometer. Data acquisition was accomplished using a SAM 550 data system and a Digital PDP-1104 computer. The punched samples were mounted with double sided stick tape. The binding energies were referenced to the C 1s photopeak at 284.6 eV. Wide scan (0 to 1100 eV) spectra were used to identify the major elements present on the

surface of the samples. Samples were scanned repetitively to obtain the atomic fractions of elements present in the sample surface.

RESULTS AND DISCUSSION

X-ray Photoelectron Spectroscopy (XPS)

The XPS results for the fractured lap shear samples where the Ti 6-4 adherends were pretreated by the Pasa Jell process are summarized in Table II. The values of the binding energy (B.E.) in eV and atomic percent (A.P.) for each photopeak are listed. Sample Nos. 056-P-32, 47 and 49 failed cohesively. The 'A' and 'B' designation in Table II refers to the two fracture surfaces for each of these samples. Since the samples failed cohesively, the XPS results for the two surfaces should be quite similar. Indeed, this is the case as judged by the agreement between the atomic percentages.

The F 1s photopeak at an average value of 688.3 eV seen in all samples is attributed to the fluorine content of the adhesive. The O 1s photopeak at an average value of 531.6 eV is seen on all surfaces and is also due to the adhesive. The lower binding energy component at 529.2 eV on the metal failure side (MFS) of Sample No. 056-P-37 is assigned (9) to oxygen in the titanium oxide surface layer. In agreement with this assignment, a significant amount of Ti was present only on this same surface which is evidence for interfacial failure. It is important to note that no significant Ti photopeak was found on the surfaces of the other three samples which had been aged for 500, 1000 and 5000 hrs. This result is evidence of a residual adhesive film on the fracture surfaces thicker than the XPS sampling depth (5 nm) for those samples aged up to 5000 hrs. The N 1s photopeak present at an average binding energy 400.0 eV on all samples is due to the adhesive. There were no significant amounts of Cr or Ca present on these samples, in contrast to the presence of these two

elements on Pasa-Jell pretreated Ti 6-4 adherend prior to bonding (10).

The XPS results of fractured Ti 6-4 adherends which had been pretreated with 10V chromic acid anodize are summarized in Table III. The binding energies of the fluorine, oxygen, titanium and nitrogen photopeaks are similar to those reported in Table II. Ti was observed on the adhesive substrate surface (ASS) of Sample No. 056-10-65 which had been thermally aged at 450°F for 10,000 hrs. The presence of Ti on the (ASS) could have resulted from punching or a weakening of the surface oxide layer caused by long term thermal aging.

Lap Shear Strength

The lap shear strengths of Ti 6-4 adherends pretreated by the Pasa Jell process and by 10V chromic acid anodize, bonded with NR 056X and then aged at 450°F from 500 to 10,000 hrs are shown comparatively in Figure 1. The consistently lower lap shear strengths for the Pasa-Jell pretreated Ti 6-4 adherends may be due to the diminished mechanical interlock in a thinner oxide layer as reported (11) for this particular pretreatment. Indeed, after 10,000 hrs at 450°F, the 10V chromic acid anodized sample No. 056-10-65 still failed cohesively whereas the Pasa-Jell sample No. 056-P-37 failed interfacially.

Scanning Electron Microscopy (SEM)

The SEM photomicrographs of the two substrates (ASS and MSS) of Sample No. 056-10-65 which failed cohesively are shown in Figure 2 and are superimposable. The ASS of this sample appears to consist of only adhesive with a few cracks on the surface through which the scrim cloth is visible. As reported in the XPS results, this surface gave a significant Ti photopeak after aging for 10,000 hrs at 450°F which may be due to a weakening of the surface oxide layer. Patches of residual adhesive are seen on the MSS. In

contrast a SEM photomicrograph of the fracture surface of a representative cohesively failed sample (No. 056-10-60) is shown in Figure 3. It is obvious that fracture occurred within the adhesive exposing scrim cloth, some areas of which appeared not to have been wetted by the adhesive.

SUMMARY

The appearance of an XPS Ti photopeak in fractured lap shear samples which had been thermally aged was used to assign the failure mode. The lap shear strengths were consistently higher for the chromic acid anodized (10V) Ti 6-4 adherends than for the Pasa-Jell pretreatment. Interfacial failure was observed only for the Pasa-Jell pretreated Ti 6-4 which had been aged for 10,000 hrs at 450°F.

ACKNOWLEDGEMENTS

Research supported under NASA Grant NAG 1-252. We recognize the expertise of Frank Cromer and Lilly Fainter in the XPS and SEM analyses.

REFERENCES

- (1) C. L. Hendricks, "Evaluation of High Temperature Structural Adhesives for Extended Service", Contract NAS1-15605, June 1979, page 27-36.
- (2) Anne K. St. Clair and Terry L. St. Clair, "The Development of Aerospace Polyimide Adhesives", NASA Technical Memorandum 84587, January 1983, page 13,16.
- (3) P. M. Hergenrother, "PPQ's Containing Pendent Ethynyl and Phenylethynyl Groups," NASA Tech Briefs, Spring/ Summer 1982, page 396.
- (4) W. L. Baun, "Surface Characterization of Titanium and Titanium Alloys, Part II: Effect on Ti-6Al-4V Alloy of Laboratory Chemical Treatments," Technical Report AFML-TR-76-29, Part II, May 1976.

- (5) J. D. Venables, D. K. McNamara, J. M. Chen, B. M. Ditchek, T. I. Morgenthaler and T. S. Sun, "Effect of Moisture in Adhesively Bonded Aluminum Structures" in Proc. of 12th Natl. SAMPE Techn. Conf., M. Smith, Ed., pp 909-923, SAMPE, Azusa, CA (1980).
- (6) M. Natan and J. D. Venables, "The Stability of Anodized Titanium Surfaces in Hot Water", J. Adhesion, 15, 125-136 (1983).
- (7) P. D. Peters, C. L. Hendricks, E. A. Ledbury, "Failure Analysis and Surface Characterization of Thermally Aged Bonded Ti", Abstracts, 56th Colloid and Surface Science Symposium, Blacksburg, VA, June, 1982.
- (8) A. V. Pocius, D. A. Wangsness, C. J. Almer and A. G. McKown, "Durability of Structural Adhesives as Determined by the Sustained Load Shear Test", Abstracts, 185th Am. Chem. Soc. Meetg., Seattle, WA, March, 1983.
- (9) J. G. Mason, R. Siriwardane and J. P. Wightman, "Spectroscopic Characterization of Acidity of Titanium (6% Al-4% V) Surfaces", J. Adhesion, 11, 315-328 (1981).
- (10) W. Chen, R. Siriwardane and J. P. Wightman, "Spectroscopic Characterization of Ti 6-4 Surfaces after Chemical Pretreatment", in Proc. of 12th Natl. SAMPE Techn. Conf., M. Smith, Ed., pp. 896-908, SAMPE, Azusa, CA (1980).
- (11) M. Natan, K. R. Breen and J. D. Venables, Technical Report MML TR 82-20c, Martin Marietta Labs., Baltimore, MD (1982).

TABLE I

DESCRIPTION OF BOEING T1 6-4 FRACTURED LAP SHEAR SAMPLES

<u>Sample No.</u>	<u>Surface Pretreatment</u>	<u>Time (hrs)[Temp]</u>	<u>Lap Shear Strength(psi)</u>	<u>Failure Mode*</u>
056-10-60	10V CAA	500[450°]	1590	Cohesive
056-10-20	10V CAA	1000[450°]	1830	Cohesive
056-10-63	10V CAA	5000[450°]	2220	Cohesive
056-10-65	10V CAA	10000[450°]	1760	Cohesive
056-P-32	PASA JELL	500[450°]	1220	Cohesive
056-P-47	PASA JELL	1000[450°]	1250	Cohesive
056-P-49	PASA JELL	5000[450°]	880	Cohesive
056-P-37	PASA JELL	10000[450°]	540	Interfacial

*based on XPS analysis of Ti 2p3 photopeak.

TABLE II
XPS ANALYSIS OF FRACTURED BOEING T1 6-4 LAP SHEAR
SAMPLES BONDED WITH NR 056X

Sample No. Photopeak	056-P-32(A)		056-P-32(B)		056-P-47(A)		056-P-47(B)	
	B.E.	A.P.	B.E.	A.P.	B.E.	A.P.	B.E.	A.P.
F 1s	688.4	11.3	688.2	12.3	688.2	10.9	688.2	12.4
O 1s	532.0	8.7	531.6	9.8	531.8	11.2	531.6	10.6
Ti 2p3		NSP		NSP		NSP		NSP
N 1s	400.2	3.8	400.2	4.2	400.2	3.3	400.0	4.2
C 1s	284.6	75.7	284.6	73.2	284.6	73.6	284.6	72.1

Sample No. Photopeak	056-P-49(A)		056-P-49(B)		056-P-37(AFS)		056-P-37(MFS)	
	B.E.	A.P.	B.E.	A.P.	B.E.	A.P.	B.E.	A.P.
F 1s	688.2	12.3	688.0	10.3	688.4	4.1	687.6	13.4
O 1s	531.8	9.7	531.6	11.3	532.0	9.8	531.2 529.2	16.6
Ti 2p3		NSP		NSP		NSP	457.6	1.7
N 1s	400.0	4.4	400.0	4.3	400.0	2.7	399.8	2.9
C 1s	284.6	73.1	284.6	73.4	284.6	82.1	284.6	64.2

NSP - no significant peak

TABLE III

XPS ANALYSIS OF FRACTURED BOEING T1 6-4 LAP SHEAR SAMPLES
BONDED WITH 056

Sample No. photopeak	056-10-60(A)		056-10-60(B)		056-10-20	
	B.E.	A.F.	B.E.	A.F.	B.E.	A.F.
F 1s	688.2	11.5	688.2	4.1	688.2	11.2
O 1s	531.8	11.4	532.0	16.9	531.6	11.6
Ti 2p3		NSP		NSP		NSP
N 1s	400.0	3.2	400.2	1.9	400.2	3.6
C 1s	284.6	72.9	284.6	76.1	284.6	72.2

Sample No. Photopeak	056-10-63A)		056-10-65(ASS)		056-10-65(MSS)	
	B.E.	A.P.	B.E.	A.P.	B.E.	A.P.
F 1s	688.2	11.7	688.0	12.3	688.2	10.9
O 1s	531.8	13.3	531.4	12.5	531.4 529.8	20.1
Ti 2p3		NSP	458.6	0.5	458.2	3.7
N 1s	400.0	3.7	399.8	4.5	400.0	3.0
C 1s	284.6	69.8	284.6	69.4	284.6	61.3

NSP - no significant peak

ORIGINAL PAGE IS
OF POOR QUALITY

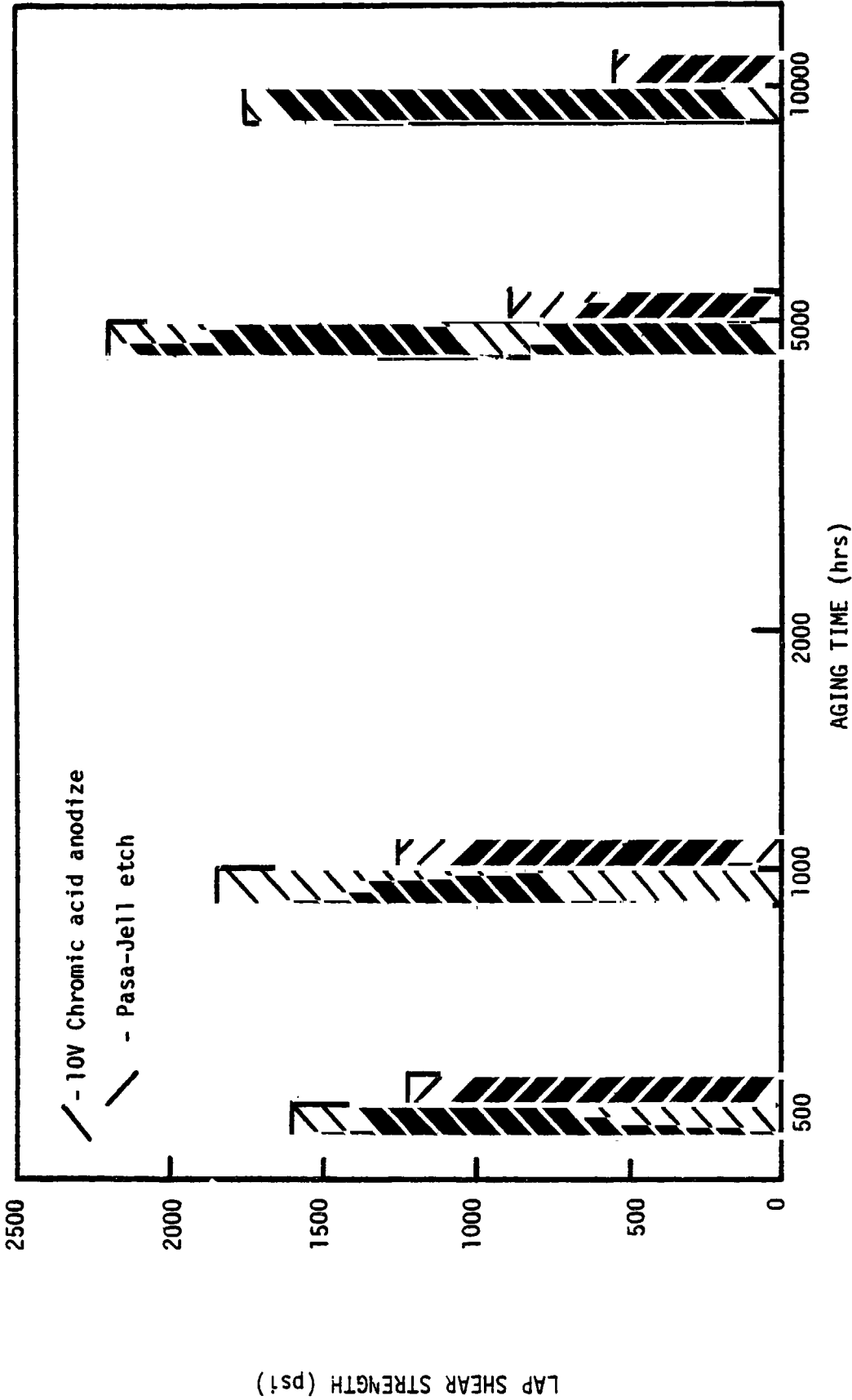
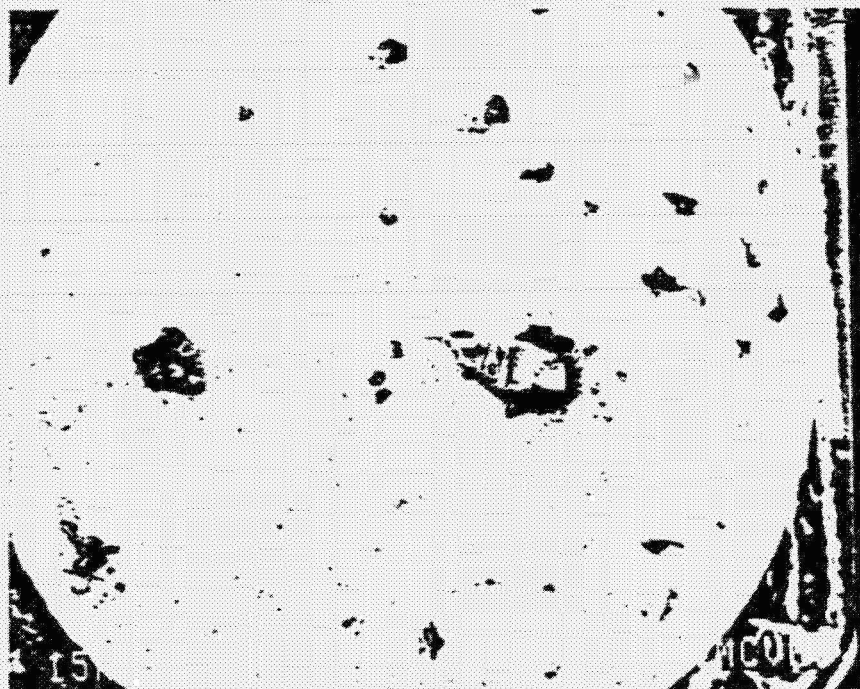


Figure 1. Lap shear strengths for 056X bonded Ti 6-4 adherends pretreated by 10V chromic acid anodize and by Pasa-Jell etch as a function of aging time at 450°F.



A



B

Figure 2. SEM photomicrographs of (A) adhesive substrate surface and (B) metal substrate surface for Sample No. 056-10-65.

ORIGINAL PAGE IS
OF POOR QUALITY



Figure 3. SEM photomicrograph of adhesive failure surface for
Sample No. 056-10-60.

SEM/XPS ANALYSIS OF FRACTURED ADHESIVELY BONDED Ti 6-4 SAMPLES.

II. POLYPHENYLQUINOXALINE (PPQ).

Surani S. Dias and J. P. Wightman
Chemistry Department
Center for Adhesion Science
Polymer Materials and Interfaces Laboratory
Virginia Polytechnic Institute and State University
Blacksburg, VA 24061

INTRODUCTION

The development of high temperature structural adhesives with improved strength and durability for adhesive bonding of Ti metals is an important study for the advanced aircraft industry in the U.S.A. Previous studies have indicated the importance of the surface oxide layer on Ti 6-4 for bond durability (1,2). A review of the surface oxide layer on Ti 6-4 have been reported (3).

Most commercially available high temperature adhesives such as FM-34 and NR150B2G are good for short term small area bonding at 600°F (4). However good processing, mechanical and thermal properties have been shown by PPQ (polyphenylquinoxaline) adhesive at 600°F. Furthermore, the trace amounts of solvents left on the PPQ serve as a plasticizer to enhance their processibility (4).

The objective of this research is the characterization of the fracture surfaces of Ti 6-4 lap shear coupons bonded with PPQ adhesive and thermally aged up to 10,000 hours. The lap shear strength of these samples have been reported (5).

EXPERIMENTAL

Samples

Fractured Ti 6-4 lap shear samples were sent from the Boeing Aerospace Company and these panels were used as received. A detailed microscopic/spectroscopic study of similar samples including crack extension measurements has been reported (6). The samples used in this study are described in Table I. It is noted that these samples are quite interesting because few bond durability studies have extended to 10,000 hrs at 450°F. The Ti 6-4 adherends were pretreated by both 10V and 5V chromic acid anodize (CAA) and by a Boeing phosphate-fluoride (PF) etch. The Ti 6-4 panels were bonded with PPQ (polyphenylquinoxaline). The polyphenylquinoxaline (PPQ) is formed by reacting 3,3',4,4'-tetraaminobiphenyl with 1,3-Bis(phenylglyoxalyl)/benzene in a 1:1 mixture of m-cresol and xylene at 298°K (77°F). Furthermore, this high molecular weight-high temperature thermoplastic does not undergo a chemical cure reaction (7,8).

The fractured Ti 6-4 surfaces were categorized based on XPS analysis as cohesive or interfacial mode failure as listed in Table I. A 1/4" diameter sample was punched after visual examination of both fracture surfaces. These punched samples were then assigned to the following groups: metal failure surface (MFS), adhesive failure surface (AFS), metal substrate surface (MSS), and adhesive substrate surface (ASS). These four surfaces are shown schematically in Figure 1. A Bausch and Lomb stereo-zoom optical microscope (OM) was used to photograph each punched sample at 20X.

Scanning Electron Microscopy (SEM)

The samples were mounted with copper tape on an aluminum stub. One set of samples was coated with a gold/palladium alloy and photomicrographs at various magnifications were obtained on an AMR (Advanced Metal Research

Corporation: Model 900) scanning electron microscope. A second set of samples was gold-coated and photomicrographs of these specimens were obtained using a JEOL JFM 35c scanning electron microscope. The surface of some of the samples were coated with carbon and were examined by EDX (energy dispersive x-ray analysis) in order to identify the elements present in that particular surface.

X-ray Photoelectron Spectroscopy (XPS)

The XPS studies of the fractured samples were done using a Physical Electronics ESCA/SAM Model 550 electron spectrometer. Data acquisition was accomplished using a SAM 550 data system and a Digital PDP-1104 computer. The punched samples were mounted with double sided stick tape. The binding energies were referenced to the C 1s photopeak at 284.6 eV. Wide scan (0 to 1100 eV) spectra were used to identify the major elements present on the surface of the samples. Samples were scanned repetitively to obtain the atomic fractions of elements present in the sample surface.

RESULTS AND DISCUSSION

Scanning Electron Microscopy/Optical Microscopy(SEM/OM)

Extensive microscopy work was done on the samples listed in Table I. However, microscopy is reported for only two samples representative of cohesive and interfacial failure. A photograph of the fractured lap shear Sample No. PPQ-10-46 which failed cohesively is shown in Figure 2A. An OM photomicrograph of a sample punched from the indicated region of Side I is shown in Figure 2B. An SEM photomicrograph of the same sample is shown in Figure 2C. The cohesive failure of this sample involved extensive disruption of the glass scrim cloth. No features characteristic of the Ti 6-4 adherend are seen in the SEM photomicrograph. EDX analysis of this sample showed only Ca and Si signals characteristic of glass.

In contrast, SEM photomicrographs for Sample No. PPQ-D-5 which failed interfacially are shown in Figure 3. The adhesive failure surface (AFS) and the metal failure surface (MFS) are shown in Figures 3A and 3B, resp. Features characteristic of the acid etched phosphate-fluoride pretreated Ti 6-4 surface (9) are seen in Figure 3B. Imprints of the β -phase of the alloy are clearly seen in the adhesive of the adhesive failure surface (AFS) in Figure 3A. The metal substrate surface (MSS) is shown at higher magnification in Figure 3D. Again the imprint of this surface is seen in the adhesive on the adhesive substrate surface (ASS) in Figure 3C, as evidenced by the voids left by pull-out of the β -phase.

XPS Analysis

The results of an extensive XPS analysis of the different fractured surfaces are shown in Tables II-IV. A few general comments on the XPS results are appropriate. A N 1s photopeak at an average binding energy of 399.0 ± 0.1 eV was observed on all samples. The Ca and Si photopeaks observed on a number of surfaces probably resulted from exposed scrim cloth (see Figure 2). However, there is some evidence to suggest that the sizing on the scrim cloth is thermally degraded on aging and may in fact migrate into the interphase region. The evidence is that a Si photopeak is observed on some metal surfaces, for example, PPQ-10-36, where no glass fibers are seen in the SEM (see Figures 3B and 3D) and where no Si signal is observed in the EDX spectrum. A recent report (10) notes evidence for glass wool bleed in gas chromatographic columns. Additional experiments are needed to determine if indeed the scrim cloth sizing is degraded on thermal aging which in turn results in diminished bond durability.

The Pb photopeak noted on nine surfaces is associated with the polyphenylquinoxaline adhesive. Lead is not present on the surface of neat PPQ film but appears in the fracture surface(s) of a number of thermally aged

samples bonded with PPQ. Lead is not observed on the pretreated Ti 6-4 surface prior to bonding or on any fracture surfaces bonded with either NR-056 or LARC-13.

Cr 2p and F 1s photopeaks were observed on chromic acid anodized Ti 6-4 adherends prior to bonding; further, P 2p and F 1s photopeaks were observed on phosphate-fluoride pretreated Ti 6-4 adherends prior to bonding (9). It is significant that no Cr, F or P photopeaks were observed on any of the fracture surfaces analyzed. This result is expected for those samples which failed cohesively. However such photopeaks were expected to be present either on the metal failure surface (MFS) or on metal substrate surface (MSS) or both. The fact that these photopeaks were not observed on either metal surface suggests migration of these residuals into the adhesive or further into the oxide layer. Since the effective XPS sampling depth is only about 5 nm, significant migration has occurred to at least that extent. There is a difficult question to answer concerning trace residuals and that is the effect (if any) that such residuals play in determining the durability of titanium adhesive bonds. It has been reported (11) that the presence of fluorine is detrimental to adhesive bonding in aluminum. No such conclusion has been made about Ti bonding. For example, is the presence of Si, Pb, F and other trace residuals detrimental to the durability of Ti bonds? Definitive experiments are needed in this area which is difficult since it is hard to significantly alter residual concentrations without at the same time altering other properties of the adherend surface.

Sample Nos. PPQ-10-67 and PPQ-10-14 - These 10 volt chromic acid anodized samples thermally aged at 120°F for 500 and 5000 hrs respectively failed cohesively with high lap shear strength (see Table I). An O 1s photopeak from the polymer is seen at an average binding energy of 532.4 ev which is

characteristic of the PPQ adhesive. A trace amount of Ti is present on Sample No. 67 but was not observed on Sample No. 14.

Sample No. PPQ-10-46 - This 10 volt chromic acid anodized sample was thermally aged at 450°F for 500 hrs failed cohesively. Again, only a trace amount of Ti was present on the fracture surface.

Sample No. PPQ-10-36 - The adhesive failure surface (AFS) gave only a trace Ti signal for this low strength sample (910 psi) after thermal aging at 450°F for 10,000 hr. The metal failure surface (MFS) contained a fair amount of PPQ adhesive as evidenced by the doublet oxygen 1s photopeak. The XPS results for the adhesive substrate (ASS) and metal substrate (MSS) surfaces parallel those for the failure surfaces. A significant Pb photopeak is noted on three of the fracture surfaces of this sample. The fact that Pb is observed on the metal failure surface (MFS) suggests a transfer of Pb from the adhesive to the interphase.

Sample No. PPQ-A-7 - This unaged sample failed cohesively having a high lap shear strength of 4650 psi. The XPS analysis of this sample gave a single O 1s photopeak at 532.6 ev characteristic of PPQ.

Sample No. PPQ-5-28 - This sample was thermally aged at 120°F for 5000 hrs. and failed interfacially with a lap shear strength of 1780 psi. An O 1s photopeak at 532.1 ev due to the polymer is seen for both MFS and AFS. However a lower binding energy unresolved O 1s photopeak on the MFS is evidence for the surface oxide covered by a thin adhesive layer. This assignment is supported by the presence of Ti 2p₃ photopeak in the MFS.

Sample No. PPQ-5-18 and PPQ-5-8 - These samples were thermally aged at 450°F for 500 hrs. and 10,000 hrs. respectively. The Sample No. 8 aged for 10,000 hrs. failed interfacially and has a low lap shear strength of 420 psi. As expected a strong Ti photopeak is shown on both MFS samples. However, a

significant amount of Ti was also present on the AFS for the Sample No. 8 that was thermally aged to 10,000 hrs. This is an interesting finding because the sample thermally aged at 120°F for 5000 hrs showed no trace of Ti on the AFS. This result suggests the cracking of the oxide layer on the Ti 6-4 adherend and transfer of the metal oxide to the AFS with long term aging at 450°F.

Furthermore, only a trace amount of Si is present on the MFS of Sample No. 28 [120°F, 5000 hrs]. However a significant amount of Si is present on the MFS side for both Sample Nos. 18 and 8. No significant peaks of Si are found on any of AFS of the above samples. This suggests a transfer of Si from the glass cloth to the metal surface with thermal aging at higher temperatures. A significant amount of Pb is found on all the samples including those discussed above and presumably is introduced in the polymer synthesis.

Sample No. PPQ-D-5 - This phosphate fluoride pretreated sample was thermally aged at 25°C and failed interfacially with a lap shear strength of 1950 psi. A strong O 1s photopeak from the polymer is seen for both AFS and ASS at an average binding energy of 532.5 ev. The lower O 1s photopeak at an average binding energy of 530.0 ev is due to the surface oxide layer on MFS and MSS. This is also supported by a significant Ti 2p₃ photopeak at an average binding energy of 458.7 ev on these same surfaces. Again a significant amount of Pb from the adhesive is present on the ASS and the MSS.

Sample No. PPQ-D-4 - This sample has thermally aged at 450°F and failed cohesively with a high lap shear strength. As mentioned in the previous case, the higher energy O 1s photopeak from the polymer is seen on all surfaces whereas the lower binding energy O 1s photopeak from the surface oxide is present only on MSS.

Effect of Pretreatment, Aging Temperature and Aging Time on Failure Mode

The effect of pretreatment at constant aging time and temperature may be

seen on comparison of Sample Nos. PPQ-10-14 and PPQ-5-28 and of Sample Nos. PPQ-10-46 and PPQ-5-18. The 10V CAA pretreatment leads to cohesive failure in both cases whereas the 5V CAA pretreatment results in interfacial failure. The effect of aging temperature for 10V CAA after 500 hrs at 120°F and 450°F is seen on comparison of Sample Nos. PPQ-10-67 and PPQ-10-46. After this relatively short exposure, there is no significant effect of aging temperature on failure mode. The effect of aging time for 10V CAA at 120°F is seen on comparison of Sample Nos. PPQ-10-67 and PPQ-10-14; there is no difference between 500 and 5000 hrs. However, at 450°F, the failure mode shifts from cohesive to interfacial failure for aging at 500 versus 10,000 hrs for the 10V CAA Sample Nos. PPQ-10-46 and PPQ-10-36. Summarily, 10V CAA pretreated Ti 6-4 lap shear Samples aged for 5000 hrs at 450°F still show cohesive failure. However, longer term aging to 10,000 hrs results in interfacial failure.

SUMMARY

SEM/XPS analysis of fractured PPQ bonded Ti 6-4 lap shear samples is useful in establishing the failure mode. The 10V CAA pretreatment is superior to the 5V CAA based on failure analysis of samples aged for times up to 10,000 hrs and at temperatures up to 450°F. The XPS results suggest a weakening of the surface oxide layer with long term thermal aging. The effect, if any, of silicon and lead observed as trace residuals on the failure mode is uncertain.

ACKNOWLEDGEMENT

Research supported under NASA Grants NSG-1124 and NAG 1-252. We recognize the experimental assistance of Betty Beck.

REFERENCES

- (1) W. L. Baun, "Surface Characterization of Titanium and Titanium Alloys, Part II: Effect on Ti-6Al-4V Alloy of Laboratory Chemical Treatment", Technical Report AFML-TR-76-29, Part II, May 1976.

- (2) J. P. Venables, D. K. McNamara, J. M. Chen, B. M. Ditchek, T. I. Morgenthaler and T. S. Sun, "Effect of Moisture on Adhesively Bonded Aluminum Structures" in Proc of 12th Natl. SAMPE Techn. Conf., M. Smith Ed., pp 909-923, SAMPE, Azusa, CA (1980).
- (3) J. A. Skiles et al., manuscript to be submitted to J. Adhesion.
- (4) P. M. Hergenrother, "High-Temperature Composite Bonding with PPQ", Adhesives Age, pp. 38-43, Dec., 1977.
- (5) C. L. Hendricks, "Evaluation of High Temperature Structural Adhesives for Extended Service", Contract NASI-15605, June 1979, page 27-36.
- (6) S. G. Hall, P. D. Peters, and C. L. Hendricks, NASA Contractor Report 165944, NASA-Langley Research Center, Hampton, VA, July, 1982.
- (7) P. M. Hergenrother, "Adhesive and Composite Evaluation of Acetylene-Terminated Phenylquinoxaline Resins", Polymer Engineering and Science, 21, No. 16., Nov., 1981.
- (8) P. M. Hergenrother, "Poly(phenylquinoxalines) Containing Phenylethynyl groups", Macromolecules, 14. 898-904 (1981).
- (9) W. Chen, R. Siriwardane and J. P. Wightman, "Spectroscopic Characterization of Ti 6-4 Surface After Chemical Pretreatment", in Proc. of 12th Natl. SAMPE Techn. Conf., M. Smith, Ed., pp. 896-908, SAMPE, Azusa, CA (1980).
- (10) J. L. Daft, "Reduction of Glass Wool Bleed in GC, Am. Labr., pp 94-95, July, 1983.
- (11) J. D. Venables, private communication, 1983.

TABLE I

DESCRIPTION OF BOEING TI 6-4 FRACTURED LAP SHEAR SAMPLES

<u>Sample No.</u>	<u>Surface Pretreatment</u>	<u>Aging Time(hrs)[Temp]</u>	<u>Lap Shear Strength, psi</u>	<u>Failure mode</u>
PPQ-10-67	10 Volt CAA	500 [120°F]	2850	Cohesive
PPQ-10-14	10 Volt CAA	5000 [120°F]	2920	Cohesive
PPQ-10-46	10 Volt CAA	500 [450°F]	2560	Cohesive
PPQ-10-36	10 Volt CAA	10,000 [450°F]	910	Interfacial
PPQ-A-7	5 Volt CAA		4650	Cohesive
PPQ-5-28	5 Volt CAA	5000 [120F°]	1780	Interfacial
PPQ-5-18	5 Volt CAA	500 [450F°]	2030	Interfacial
PPQ-5-8	5 Volt CAA	10,000 [450°F]	420	Interfacial
PPQ-D-5	PF (Boeing)		1950	Interfacial
PPQ-D-4	PF (Boeing)		3000	Cohesive

Table II
 XPS ANALYSIS OF FRACTURED BOEING TI 6-4 (10V CAA) LAP SHEAR SAMPLES
 BONDED WITH PPQ

<u>Sample No.</u> <u>Photopeak</u>	PPQ-10-67		PPQ-10-14		PPQ-10-46	
	<u>B.E.</u>	<u>A.F.</u>	<u>B.E.</u>	<u>A.F.</u>	<u>B.E.</u>	<u>A.F.</u>
O 1s	532.4	0.13	532.4	0.153	532.4	0.18
Ti 2p _{3/2}	458.6	0.001		NSP	458.4	0.001
Ca 2p _{3/2}		NS	348.2	0.008		NS
Pb 4f _{7/2}		NS		NSP		NS
Si 2p	102.4	0.040	103.0	0.049	102.8	0.046

<u>Sample No.</u> <u>Photopeak</u>	PPQ-10-36(AFS)		PPQ-10-36(MFS)		PPQ-10-36(ASS)		PPQ-10-36(MSS)	
	<u>B.E.</u>	<u>A.F.</u>	<u>B.E.</u>	<u>A.F.</u>	<u>B.E.</u>	<u>A.F.</u>	<u>B.E.</u>	<u>A.F.</u>
O 1s	532.2	0.15	531.8 _D	0.33	532.4	0.14	532.2 _D	0.28
Ti 2p _{3/2}	458.6	trace	458.2	0.028		NSP	458.4	0.03
Ca 2p _{3/2}		NSP		NSP		NSP		NSP
Pb 4f _{7/2}	138.6	0.005	138.1	0.017	138.8	0.005		NSP
Si 2p	102.0	0.005	102.0	0.014	102.2	0.011	102.6	0.09

Table III

XPS ANALYSIS OF FRACTURED BOEING TI 6-4 (5V CAA) LAP SHEAR SAMPLES
BONDED WITH PPQ

<u>Sample No.</u> <u>Photopeak</u>	PPQ-A-7		PPQ-5-28(AFS)		PPQ-5-28(MFS)	
	<u>B.E.</u>	<u>A.F.</u>	<u>B.E.</u>	<u>A.F.</u>	<u>B.E.</u>	<u>A.F.</u>
O 1s	532.6	0.17	532.2	0.108	532.0 _D	0.18
Ti 2p _{3/2}		NS		NSP	457.8	0.017
Ca 2p _{3/2}		NS		NSP		NSP
Pb 4f _{7/2}		NS	139.2	0.001	138.4	0.006
Si 2p	103.2	0.059	102.4	0.015	102.6	trace

<u>Sample No.</u> <u>Photopeak</u>	PPQ-5-18(AFS)		PPQ-5-18(MFS)		PPQ-5-8(AFS)		PPQ-5-8(MFS)	
	<u>B.E.</u>	<u>A.F.</u>	<u>B.E.</u>	<u>A.F.</u>	<u>B.E.</u>	<u>A.F.</u>	<u>B.E.</u>	<u>A.F.</u>
O 1s	532.3	0.310	532.6	0.147	532.2	0.085	530.2 _D	0.167
Ti 2p ₃		NSP	458.9	0.007	458.8	0.003	458.2	0.026
Ca 2p _{3/2}		NSP		NSP		NSP		NSP
Pb 4f _{7/2}	138.0	0.003	138.8	0.005	138.8	0.004	138.4	0.017
Si 2p		NSP	102.8	0.019		NSP	102.2	0.018

Table IV

XPS ANALYSIS OF FRACTURED BOEING TI 6-4 (BOEING PF) LAP SHEAR SAMPLES
BONDED WITH PPQ

<u>Sample No.</u> <u>Photopeak</u>	PPQ-D-5(AFS)		PPQ-D-5(MFS)		PPQ-D-5(ASS)		PPQ-D-5(MSS)	
	<u>B.E.</u>	<u>A.F.</u>	<u>B.E.</u>	<u>A.F.</u>	<u>B.E.</u>	<u>A.F.</u>	<u>B.E.</u>	<u>A.F.</u>
O 1s	532.3	0.13	530.1 531.9	0.27	532.8 _D	0.071	529.8* D	0.27
Ti 2p _{3/2}		NS	458.5	0.044	459.2	0.0037	458.9	0.070
Ca 2p _{3/2}		NS	347.1	0.0078		NS	347.5	0.012
Pb 4f _{7/2}		NS		NS	138.3	0.0014	138.6	0.0081
Si 2p	153.2	0.031	153.1	0.052		NS		NS

<u>Sample No.</u> <u>Photopeak</u>	PPQ-D-4		PPQ-D-4(ASS)		PPQ-D-4(MSS)	
	<u>B.E.</u>	<u>A.F.</u>	<u>B.E.</u>	<u>A.F.</u>	<u>B.E.</u>	<u>A.F.</u>
O 1s	532.6	0.14	532.9	0.33	530.2* D	0.28
Ti 2p _{3/2}		NS	458.4	0.0032	458.4	0.057
Ca 2p _{3/2}	348.1	0.011		NS	347.1	0.006
Pb 4f _{7/2}		NS	138.6	0.001	138.4	0.003
Si 2p	153.6	0.039		NS		NS

*lower B.E. peak predominates.

ORIGINAL PAGE #
OF POOR QUALITY

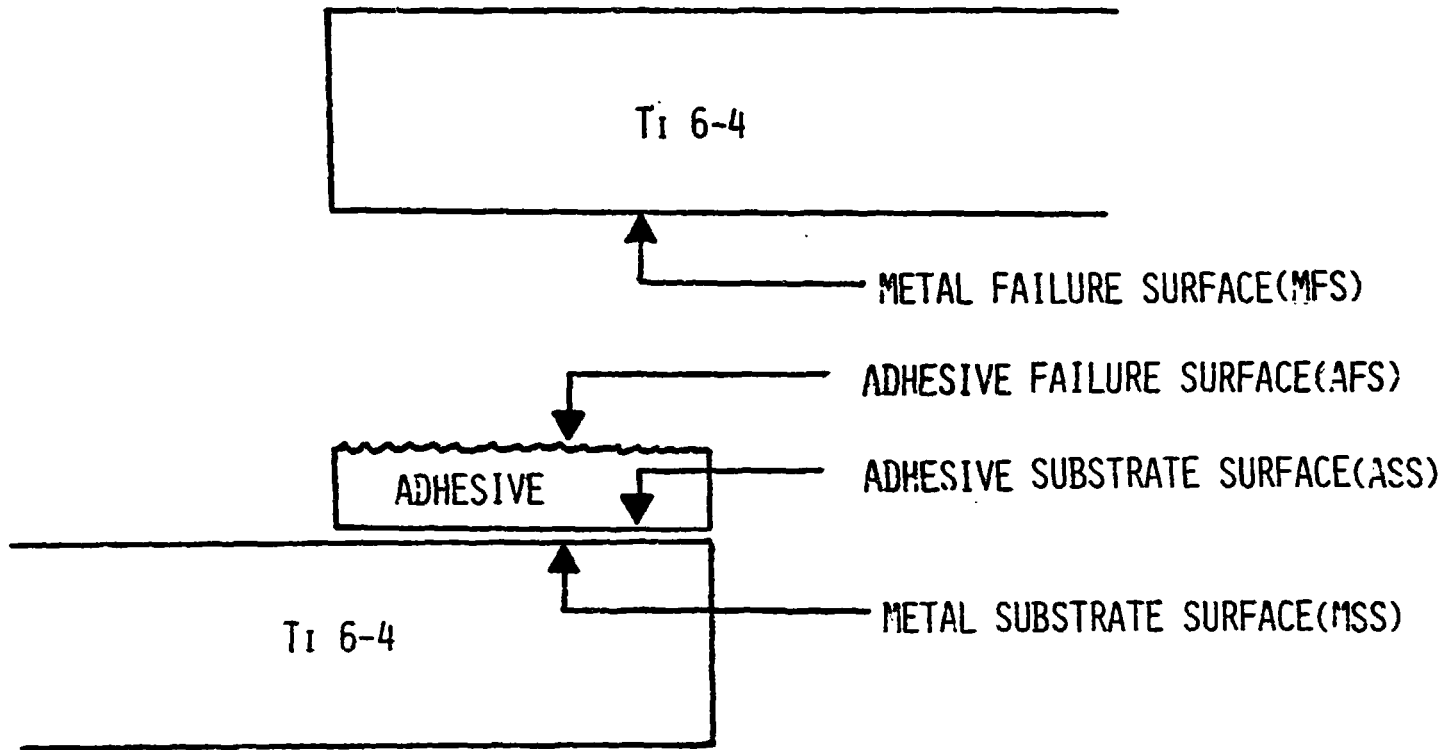
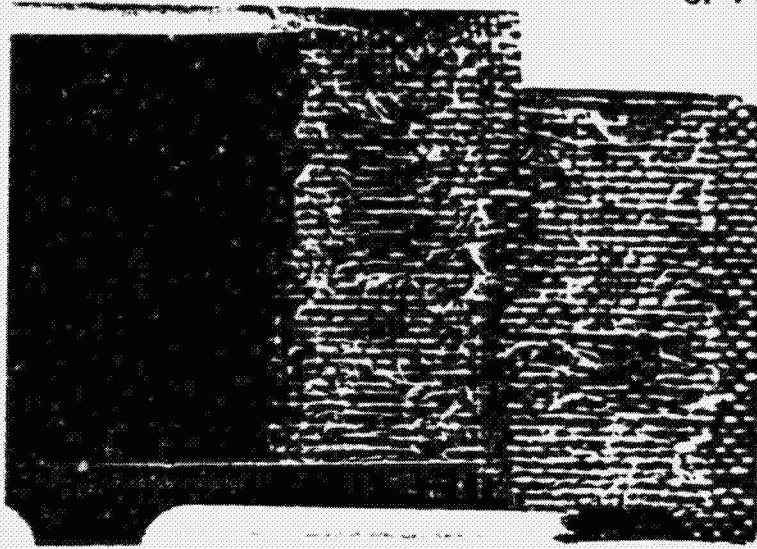


Figure 1. Schematic of fractured lap shear specimen.

ORIGINAL PAGE IS
OF POOR QUALITY



A PPAQ-10-46

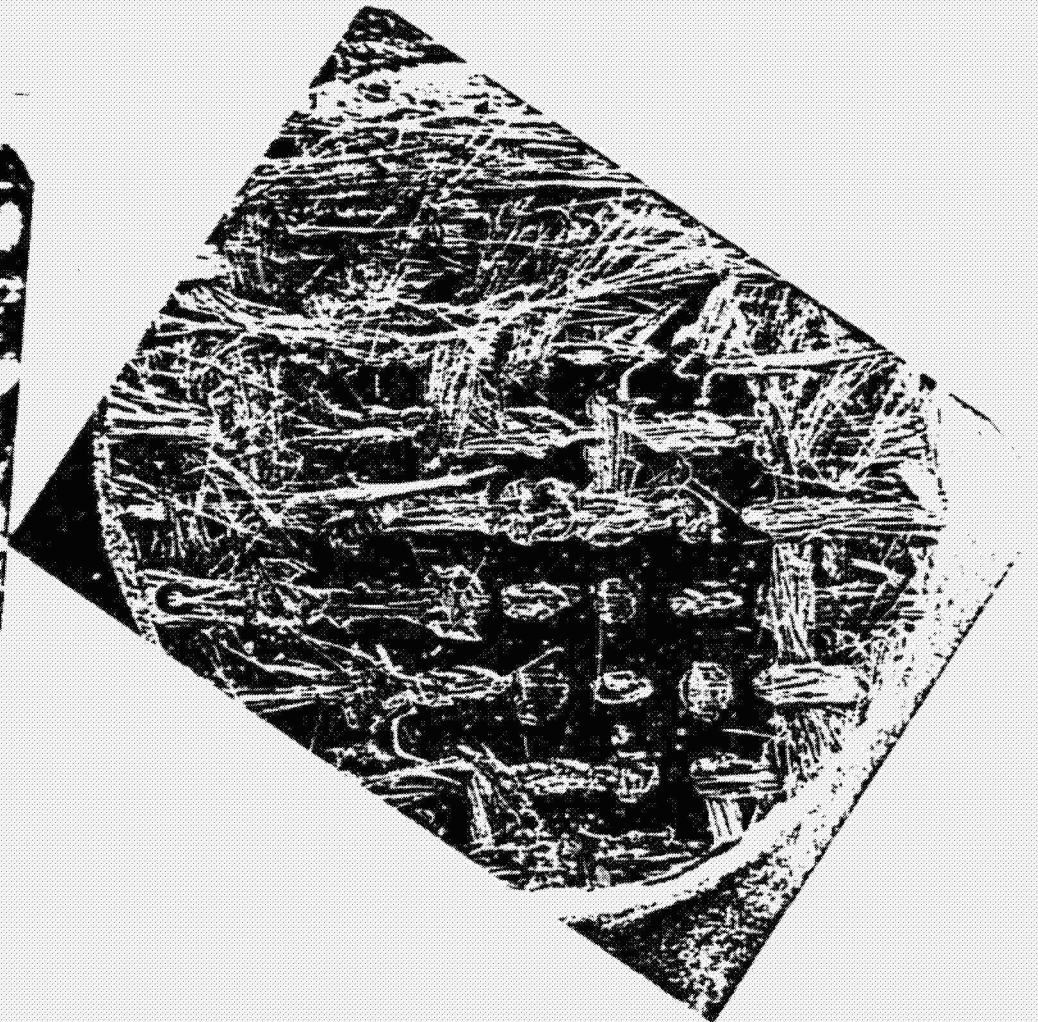
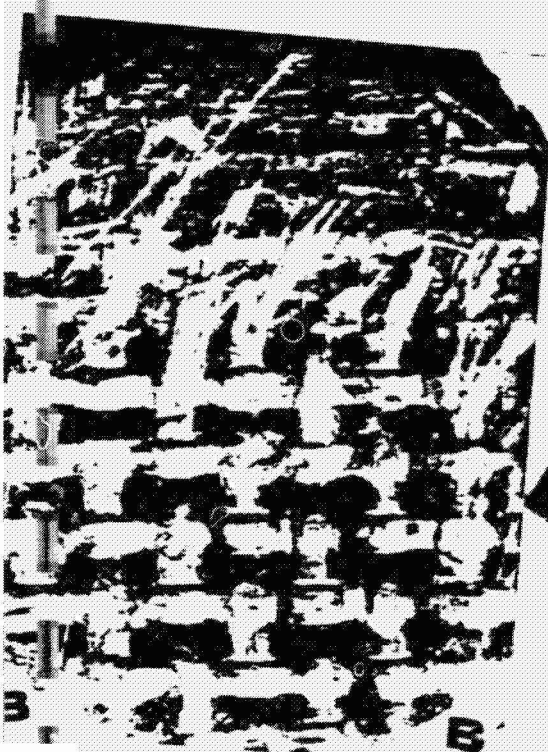
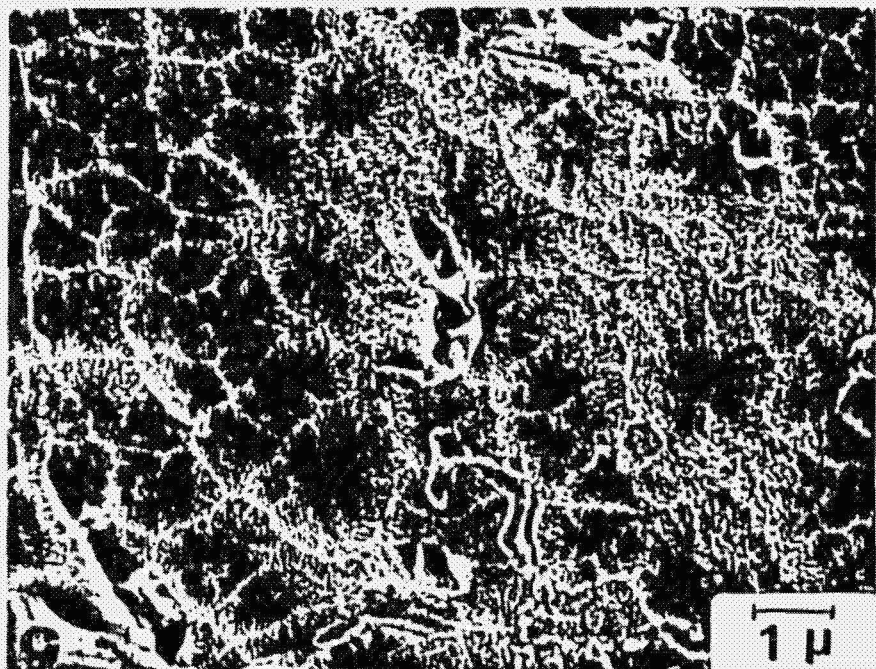
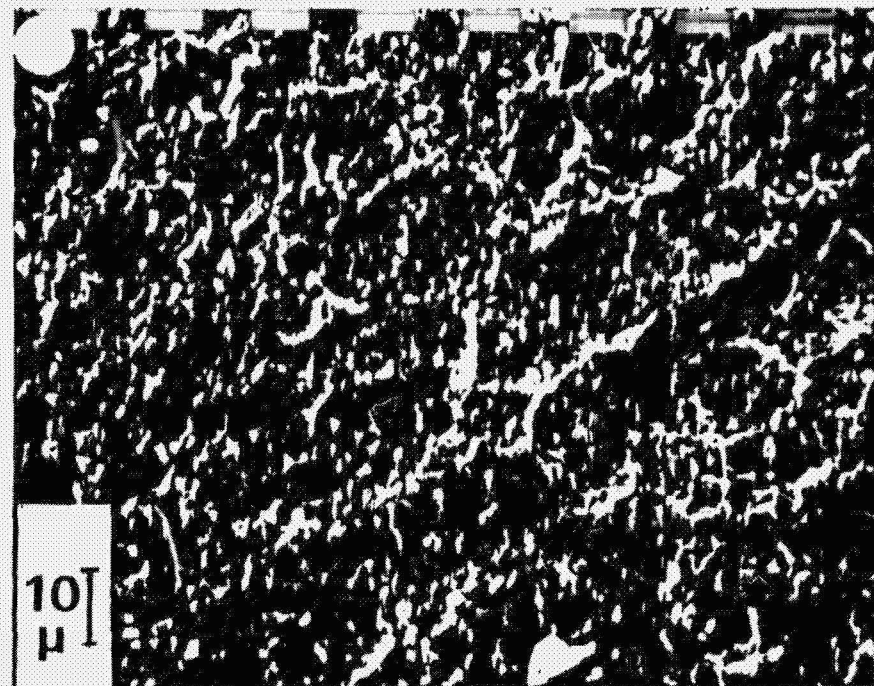
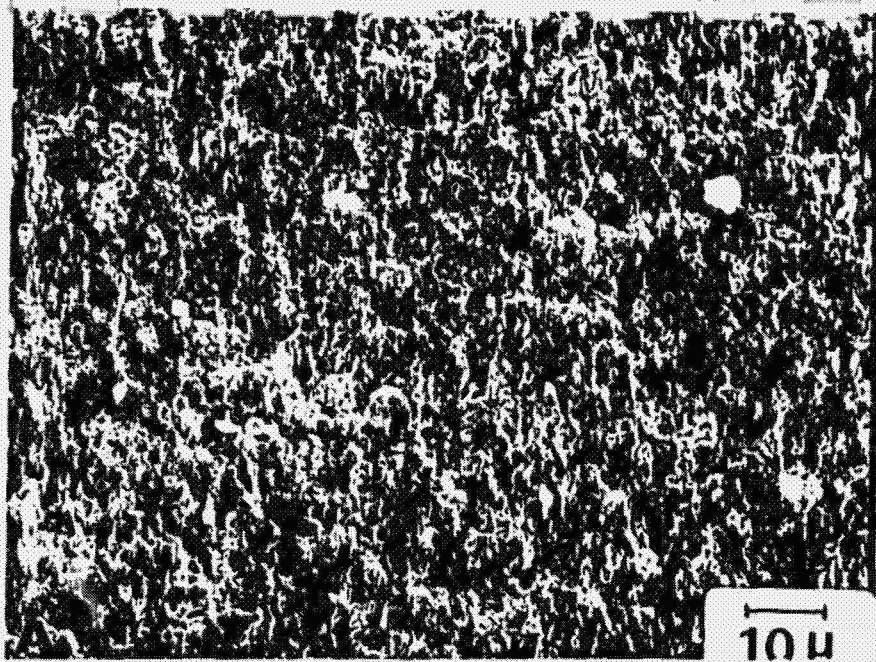


Figure 2. (A) Photograph of fractured lap shear sample (B) Optical photomicrograph of punched sample (C) SEM photomicrograph of punched sample.



ORIGINAL PAGE IS
OF POOR QUALITY

Figure 3. SEM photomicrograph of Sample No. PPQ-D-5. (A) AFS (B) MFS (C) ASS (D) MSS.

SEM/XPS ANALYSIS OF FRACTURED ADHESIVELY BONDED Ti 6-4 SAMPLES.

III. LARC-13.

Surani S. Dias and J. P. Wightman
Chemistry Department
Center for Adhesion Science
Polymer Materials and Interface Laboratory
Virginia Polytechnic Institute and State University
Blacksburg, VA 24061

INTRODUCTION

The development of high temperature durable adhesive for joining metals, fiber-reinforced/polymer-matrix composites, metal/composites and films have become increasingly important research areas for the aerospace industry. Research workers at NASA Langley have been studying linear aromatic condensation polyimides that are good candidates for aerospace adhesives because of their remarkable thermal and thermooxidative stability, toughness and flexibility, radiation and solvent resistance, low density, and excellent mechanical and electrical properties (1),

However, in recent years the LARC family of addition polyimide adhesives have been evaluated for bonding titanium and polyimide/graphite composites. LARC-13 polyimide has a high crosslink density and can be used at temperatures higher than its glass transition temperatures of 270°C (1). Furthermore, LARC-13 adhesive has been shown to be useful in the bonding of honeycomb sandwich structures which require low bonding pressures and very short bonding times at the bonding temperatures (1,2).

The objective of the present research is the SEM/XPS analysis of fractured Ti 6-4 lap shear coupons bonded with LARC-13 adhesive and thermally aged for up to 10,000 hrs. The lap shear strengths of these samples have been reported (3).

EXPERIMENTAL

Samples

Fractured Ti 6-4 lap shear samples were sent from the Boeing Aerospace Company and these panels were used as received. A detailed microscopic/spectroscopic study of similar samples including crack extension measurements has been reported (4). The samples used in this study are quite interesting because few bond durability studies (5) have extended to 10,000 hrs at 450°F. The Ti 6-4 adherends were pretreated by 10V chromic acid anodize, Pasa Jell, phosphate fluoride, (Picatinny and Boeing) and alkaline peroxide etch. The Ti 6-4 panels were bonded with LARC-13 (polyimide).

The LARC-13 polyimide is synthesized by the following general procedure: A mixture of m,m'-MDA (m,m'-diaminodiphenyl methane), NA (nadic anhydride) and BTDA (3,3',4,4'-benzophenone tetracarboxylic acid anhydride) monomers are reacted in DMF at 20°C. The resulting amic acid prepolymer is cured at 180°C to form the imide prepolymer that is further heated at 300°C to prepare the LARC-13 crosslinked polyimide (1,2,5).

The fractured Ti 6-4 surfaces were categorized either cohesive or interfacial failure based on XPS analysis [see table I]. A 3/8" diameter sample was punched after visual examination of both fracture surfaces. These punched samples were then assigned to the following groups: metal failure surface (MFS), adhesive failure surface (AFS), metal substrate surface (MSS), and adhesive substrate surface (ASS). A Bausch and Lomb stereo-zoom optical microscope (OM) was used to photograph each punched sample at 20X.

Scanning Electron Microscopy (SEM)

The samples were mounted with copper tape on an aluminum stub. One set of samples was coated with a gold/palladium alloy and photomicrographs at various magnifications were obtained on an AMR (Advanced Metal Research

Corporation: Model 900) scanning electron microscope. A second set of samples was gold-coated and photomicrographs of these specimens were obtained using a JEOL JFM 35c scanning electron microscope. The surface of some of the samples were coated with carbon and were examined by EDX (energy dispersive x-ray analysis) in order to identify the elements present in that particular surface.

X-ray Photoelectron Spectroscopy (XPS)

The XPS studies of the fractured samples were done using a Physical Electronics ESCA/SAM Model 550 electron spectrometer. Data acquisition was accomplished using a SAM 550 data system and a Digital PDP-1104 computer. The punched samples were mounted with double sided stick tape. The binding energies were referenced to the C 1s photopeak at 284.6 eV. Wide scan (0 to 1100 eV) spectra were used to identify the major elements present on the surface of the samples. Samples were scanned repetitively to obtain the atomic fractions of elements present in the sample surface.

RESULTS AND DISCUSSION

Scanning Electron Microscopy/Optical Microscopy (SEM/OM)

Extensive microscopy work was done on the samples listed in Table 1. However, microscopy is reported for only two samples, representative of cohesive and interfacial failure. A photomicrograph of the fractured lap shear Sample No. L13-10-53 which failed cohesively is shown in Figure 1. The cohesive failure of this sample involved extensive disruption of the glass scrim cloth. No features characteristic of the Ti 6-4 adherend are seen in the SEM photomicrograph. EDX analysis of this sample showed only Ca and Si signals characteristic of the glass.

In contrast, SEM photomicrographs for Sample No. L13-P-6 are shown in Figure 2. The adhesive failure surface (AFS) is shown in Fig. 2A. Adhesive-

coated scrim cloth is visible in the large void. A number of alumina particles contained in the L13 adhesive are seen in the center of the photomicrograph. The same metal failure (MFS) at increasing magnification is shown in Figs. 2B-2D. Arrows indicate areas which appear at higher magnification. Patches of adhesive are seen on the Ti 6-4 adherend of the MFS (Fig. 2B). The alumina particles in an L13 adhesive patch are seen in Fig. 2C. Features of the Ti 6-4 adherend surface are seen in Fig. 2D. In addition, there is a smooth adhesive layer covering a large area and the larger alumina particles stand in contrast to the smaller β -phase of the alloy produced by the Pasa-Jell process.

XPS Analysis

The results of an extensive XPS analysis of the different fractured surfaces are shown in Tables II and III. A N 1s photopeak at an average binding energy of 400.0 ± 0.1 eV was observed on all samples and is not included in the tables. Cr 2p and F 1s photopeaks were observed on chromic acid anodized Ti 6-4 adherends prior to bonding and further, P 2p and F 1s photopeaks were observed on phosphate fluoride pretreated Ti 6-4 adherends prior to bonding (6). It is significant that no Cr photopeak was observed on any of the fractured surfaces analyzed where the adherend had been chromic acid anodized; similarly, no P photopeak was observed for phosphate-fluoride pretreated Ti 6-4 adherend. This result is expected for those samples which failed cohesively. However, such photopeaks were expected to be present either on metal failure surfaces (MFS) or on the metal substrate surfaces (MSS) or both.

Sample Nos. L13-10-53, L13-10-41 and L13-10-28 - All these 10 volt chromic acid anodized samples were thermally aged at 120°F from 500 to 5000 hrs and failed cohesively with high lap shear strengths as listed in Table I.

As reported in Table II, a O 1s photopeak from the polymer at an average binding energy of 531.8 eV is seen on all the samples as expected for cohesive failure. A trace amount of Ti is present on Sample No. 53. However, there is no significant Ti photopeak from the rest of the samples which was expected, because failure is within the adhesive. A significant concentration of Si and Ca is present in these samples due to exposed scrim cloth. The appearance of a significant F 1s photopeak in Sample Nos. 41 and 28 is surprising, especially since no Ti photopeak was observed. This result suggests possible migration of F from the interface into the adhesive on long term (> 3000 hrs.) even at 120°F.

Sample Nos. L13-10-60, L13-10-33, L13-10-6, L13-10-21 and L13-10-50 -

These samples were thermally aged at 450° from 500 to 10,000 hrs. The two samples aged for 500 and 1000 hrs (Nos. 60 and 33) failed cohesively with high lap shear strengths. Similarly, the samples aged for 5000 and 10,000 hrs (Nos. 21 and 50) failed interfacially with lower lap shear strengths. As mentioned before the higher binding energy O 1s photopeak at about 532 eV is characteristic of the L13 adhesive on the MFS of sample and suggests a thin (< 5 nm) residual layer of adhesive on the oxide surface.

A more detailed analysis of the F 1s photopeaks demonstrate the mobility of F in the interphase. For example, no F was observed in Sample No. 60 which was aged for only 500 hrs at 450°F and which failed cohesively. However, a F 1s photopeak was observed on cohesively failed sample aged for 3000-5000 hrs at 120°F. F 1s photopeaks were observed on the fractured surfaces of Sample Nos. 33 and 6 which were aged for 1000 and 3000 hrs., respectively. Finally, no significant F 1s photopeak was observed on any of the four fractured surfaces of sample Nos. 21 and 50 which has been aged for 5000 and 10,000 hrs. respectively. It is clear then that F is labile and is migrating out of the

interfacial region and into the adhesive during thermal aging either over longer times at 120°F or shorter times at 450°F.

Sample Nos. 33 and 6 gave a higher binding energy F 1s photopeak at 688.7 ev compared to the more common F 1s photopeak at 685.6 ev. The assignment of both of these two F 1s photopeaks is uncertain. The lower binding energy peak is probably due to fluoride ion. However, the higher binding peak is yet unassigned.

As expected a significant amount of Ti is present on all MFS samples. However a significant amount of Ti is present on the AFS of Sample No. 50 that was aged at 450°F for 10,000 hrs. This is a surprising result since no titanium would be expected on the adhesive side. These results suggest the cracking of the oxide surface with long term aging at higher temperatures. Furthermore, these results are supported by the presence of a lower binding oxygen photopeak at 529.8 ev on the AFS is assigned to the surface oxide layer (7). In contrast, only a trace amount of Ti to no significant amount is present on these samples aged at 120°F.

Sample No. L13-P-25 - This sample was thermally aged at 120°F for 500 hrs failed in the mixed mode with a high lap shear strength of 2640 psi. No significant amount of either F or Ca was found on this sample. However, an intense higher binding energy C 1s photopeak is seen on both AFS and MFS. This suggests a thin layer or patches of adhesive on the MFS and is supported by the presence of a Ti 2p photopeak on MFS and also by a lower binding energy O 1s photopeaks. Furthermore, no significant amount of Ti is present on the AFS but a strong Si 2p photopeak is evident on both AFS and MFS and is due to exposed scrim cloth.

Sample No. L13-P-46, L13-P-35 and L13-P-36 - All these samples were thermally aged at 450°F for 10,000, 5000 and 10,000 hrs respectively. Sample No. 46 failed in the mixed mode with a high lap shear strength of 2280 psi whereas

both Sample Nos. 35 and 36 failed interfacially with moderate to low lap shear strengths. A trace to significant amount of F and Ca are present on these samples even after aging for 10,000 hrs at 450°F. Also a significant amount of Si is present on most of the fractured surfaces.

Furthermore, a higher binding energy O 1s photopeak is seen on most MFS, AFS and ASS surfaces. This suggests the presence of a thin layer or patches of adhesive on the MFS. Also it is interesting to note that no significant amount of Ti is present on any of the AFS which does not support the cracking of the oxide layer as in those samples pretreated by anodization.

It is significant that the Pasa-Jell pretreated Ti 6-4 adherends give only a small O 1s photopeak at the lower binding energy even on the MFS and MSS samples. This result is consistent with the low intensity Ti 2p photopeak on the same surfaces. These two results together suggest a relatively thick adhesive layer left on the Pasa-Jell treated surface.

Effect of Pretreatment, Aging Temperature and Aging Time on Failure Mode.

The effect of pretreatment at a constant aging time of 500 hrs and an aging temperature of 120°F may be seen on comparison of Sample Nos. L13-10-53 and L13-P-25; again, at 500 hrs at 450°F, a comparison is made of Sample Nos. L13-10-60 and L13-P-46. The difference is marked in that in both sets of samples, the 10V CAA pretreatment resulted in cohesive failure whereas the Pasa-Jell pretreatment resulted in interfacial failure. Both pretreatments resulted in interfacial failure at 450°F at aging times > 5000 hrs.

The effect of aging at 120°F versus 450°F for 10V CAA pretreated Ti 6-4 adherends is minimal up to 1000 hrs. However, cohesive failure was still observed at both 3000 and 5000 hrs at 120°F whereas interfacial failure occurred after 3000 hrs at 450°F.

The effect of aging time for 10V CAA pretreated Ti 6-4 adherends can be gauged at both 120°F and 450°F. Only cohesive failure is observed at 120°F on aging from 500 to 5000 hrs. However, the onset of interfacial failure at 450°F is noted between 1000 and 3000 hrs.

Comparison of Ti 6-4 Adherend Pretreatments

The results of 5V CAA, 10V CAA and Pasa-Jell pretreated Ti 6-4 adherends can be compared for three different adhesive systems, namely NR 056, PPQ and LARC 13. A consistent pattern emerges from an analysis of the XPS data for thermally aged lap shear samples. The 10V CAA pretreatment appears to be superior when compared to 5V CAA and to the Pasa-Jell process. XPS evidence has been presented to support the "cracking" of the surface oxide layer during long term thermal aging > 3000 hrs at 450°F. Siriwardane and Wightman (8) have reported calorimetric evidence on wetting by primer solutions and solvents of Ti 6-4 powders evacuated to different temperatures for a cracking of the surface oxide layer. Venables and co-workers (9) have reported the conversion of an initially amorphous TiO₂ layer following CAA to an anatase TiO₂ layer under relatively mild conditions.

There is no definitive finding concerning the role of any trace surface residuals on bond durability in any of the systems. However, several questions need to be addressed, namely (1) whether the sizing on the scrim cloth is thermally degrading, (2) whether the presence of Pb in the PPQ system is detrimental, (3) whether the labile fluorine observed in the LARC-13 adhesive is a problem.

ACKNOWLEDGEMENT

Research supported under NASA Grants NSG-1124 and NAG 1-252. We recognize the experimental assistance of Betty Beck.

REFERENCES

- (1) NASA Technical Memorandum "The Development of Aerospace Polyimide Adhesives" January 1983, page 17.
- (2) Anne K. St. Clair, Wayne S. Slomp and Terry L. St. Clair, "High-Temperature Adhesives for Bonding Polyimide Film", Adhesives Age, Jan. 1979, pp. 35-39.
- (3) C. L. Hendricks, "Evaluation of High Temperature Structural Adhesives for Extended Services", Contract NAS1-15605, June 1979, pp. 27-36.
- (4) S. G. Hall, W. D. Peters and C. L. Hendricks, NASA Contractor Report 165944, NASA-Langley Research Center, Hampton, VA, July 1982.
- (5) Anne K. St. Clair and Terry L. St. Clair, "Addition Polyimide Adhesives Containing Various Enol Groups", Polymer Engineering and Science, January, 1982, Vol. 22, No. 1.
- (6) Wen Chen, R. Siriwardane and J. P. Wightman, "Spectroscopic Characterization of Ti 6-4 Surface After Chemical Pretreatment", in Proc. of 12th Natl. SAMPE Techn. Conf., M. Smith, Ed., pp. 896-908, SAMPE, Azusa, CA (1980).
- (7) T. A. Egerton et al., Colloids and Surfaces, in press.
- (8) R. V. Siriwardane and J. P. Wightman, J. Adhesion, 15, 225-239 (1983).
- (9) J. D. Venables, private communication, 1982.

TABLE I

DESCRIPTION OF BOEING TI 6-4 FRACTURED LAP SHEAR SAMPLES

<u>Sample No.</u>	<u>Pretreatment</u>	<u>Aging Time, hrs</u> <u>[Temp.]</u>	<u>Lap Shear</u> <u>Strength, μsi</u>	<u>Failure Mode</u>
L13-10-53	10V CAA	500 [120°F]	3000	Cohesive
L13-10-54	10V CAA	1000 [120°F]	3230	Cohesive
L13-10-41	10V CAA	3000 [120°F]	2900	Cohesive
L13-10-28	10V CAA	5000 [120°F]	2810	Cohesive
L13-10-60	10V CAA	500 [450°F]	2540	Cohesive
L13-10-33	10V CAA	1000 [450°F]	2060	Cohesive
L13-10-6	10V CAA	3000 [450°F]	1250	Interfacial
L13-10-21	10V CAA	5000 [450°F]	1180	Interfacial
L13-10-50	10V CAA	10,000 [450°F]	300	Interfacial
L13-P-25	Pasa Jell	500 [120°F]	2640	Interfacial
L13-P-46	Pasa Jell	500 [450°F]	2280	Interfacial
L13-P-35	Pasa Jell	5000 [450°F]	1200	Interfacial
L13-P-36	Pasa Jell	10,000 [450°F]	700	Interfacial

TABLE II

XPS ANALYSIS OF FRACTURED BOEING TI 6-4 [10V CAA] LAP SHEAR SAMPLES
BONDED WITH LARC-13.

Sample No. Photopeak	L13-10-53		L13-10-54		L13-10-41		L13-10-28	
	B.E.	A.F.	B.E.	A.F.	B.E.	A.F.	B.E.	A.F.
F 1s		NS		NSP	685.6	0.008	686.2	0.007
O 1s	531.9	0.17	531.8	0.181	531.8	0.207	531.8	0.189
Ti 2p3	458.2	0.001		NSP		NSP		NSP
Ca 2p3		NS	347.6	0.007	347.6	0.005	347.8	0.002
Si 2p	102.6	0.036	102.6	0.027	102.2	0.022	102.2	0.009

Sample No. Photopeak	L13-10-60		L13-10-33		L13-10-6	
	B.E.	A.F.	B.E.	A.F.	B.E.	A.F.
F 1s		NSP	688.6 686.2	0.011	688.8 685.2	0.004
O 1s	531.8	0.22	531.8	0.216	531.2 _D	0.249
Ti 2p3		NSP		NSP	458.6	0.024
Ca 2p3		NSP		NSP		NSP
Si 2p	102.6	0.02	102.4	NSP		NSP

Sample No. Photopeak	L13-10-21(AFS)		L13-10-21(MFS)		L13-10-50(AFS)		L13-10-50(MFS)	
	B.E.	A.F.	B.E.	A.F.	B.E.	A.F.	B.E.	A.F.
F 1s		NSP		NSP	685.0	trace		NSP
O 1s					531.8	0.237	531.2	0.33
	532.0	0.191	531.6 _D	0.237			529.8	
Ti 2p3	458.8	0.004	458.2	0.036	458.2	0.009	458.0	0.08
Ca 2p3		NSP		NSP	347.6	0.003	346.8	0.008
Si 2p	102.0	0.035	101.8	0.023	102.0	0.004	101.6	0.014

TABLE III

XPS ANALYSIS OF FRACTURED BOEING TI 6-4 [PASA-JELL] LAP SHEAR SAMPLES
BONDED WITH LARC-13

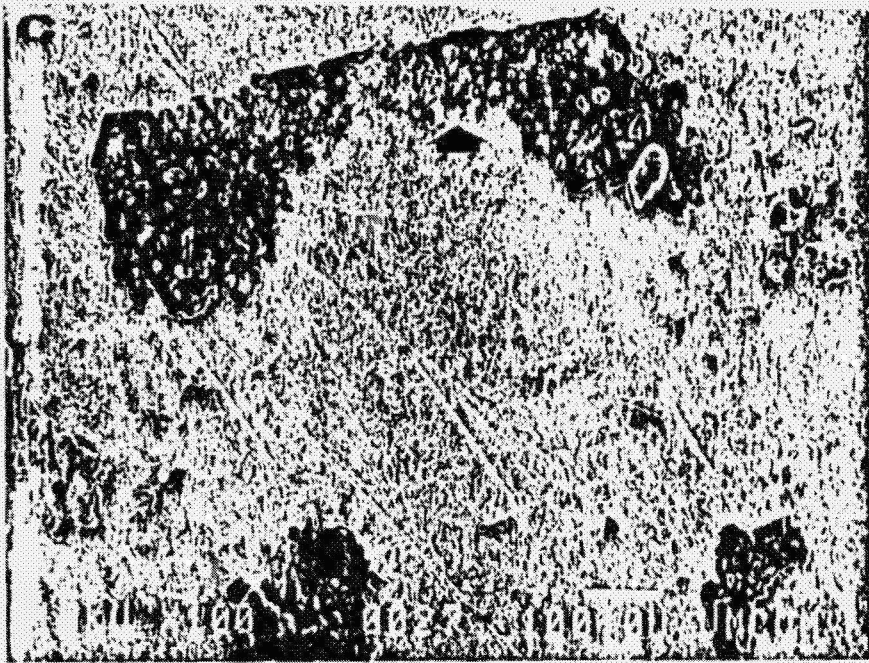
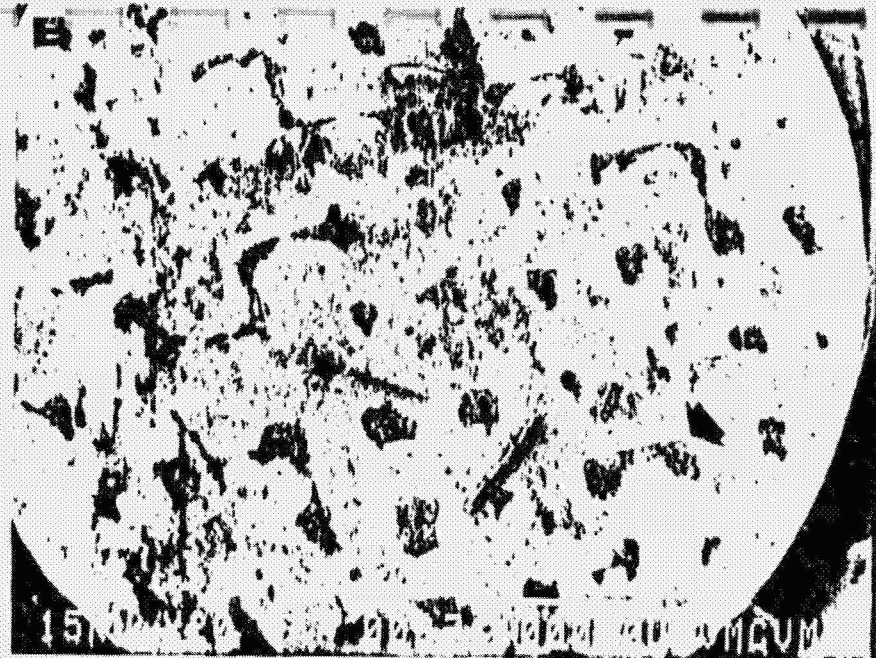
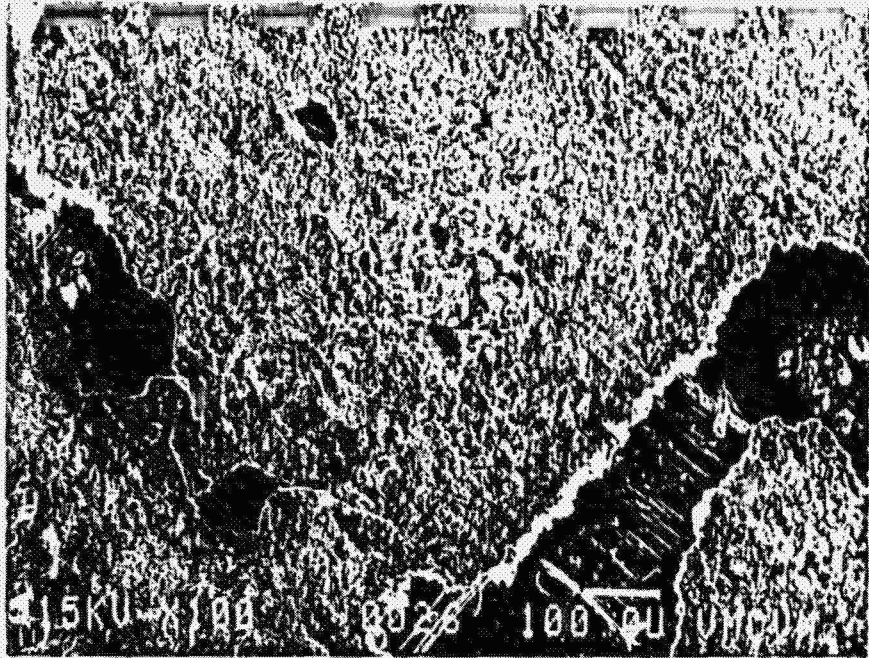
<u>Sample No.</u> <u>Photopeak</u>	<u>L13-P-25(AFS)</u>		<u>L13-P-25(MFS)</u>		<u>L13-P-46(AFS)</u>		<u>L13-P-46(MFS)</u>	
	<u>B.E.</u>	<u>A.F.</u>	<u>B.E.</u>	<u>A.F.</u>	<u>B.E.</u>	<u>A.F.</u>	<u>B.E.</u>	<u>A.F.</u>
F 1s		NSP		NSP		0.006		NSP
O 1s	531.8	0.020	531.6 ₀	0.21	531.8	0.015	532.0 ₀	0.20
Ti 2p ₃		NSP	458.4	0.008		NSP	457.6	0.009
Ca 2p ₃		NSP		NSP		NSP		NSP
Si 2p	102.6	0.027	102.2	0.009	102.6	0.003	102.4	0.028

<u>Sample No.</u> <u>Photopeak</u>	<u>L13-P-35(AFS)</u>		<u>L13-P-35(MFS)</u>		<u>L13-P-36(AFS)</u>		<u>L13-P-36(MFS)</u>		<u>L13-F-36(ASS)</u>	
	<u>B.E.</u>	<u>A.F.</u>	<u>B.E.</u>	<u>A.F.</u>	<u>B.E.</u>	<u>A.F.</u>	<u>B.E.</u>	<u>A.F.</u>	<u>B.E.</u>	<u>A.F.</u>
F 1s		NSP	688.4	trace		NSP		Trace		NSP
O 1s	531.8	0.168	531.8 ₀	0.16	531.8	0.155	531.6 ₀	0.155	532.0	0.21
Ti 2p ₃		NSP	457.8	0.008		NSP	457.6	0.012		NSP
Ca 2p ₃		NSP		NSP		NSP	346.8	NSP		NSP
Si 2p		NSP	102.2	0.024		NSP	101.6	0.022	103.0	0.023

ORIGINAL PAGE IS
OF POOR QUALITY



Figure 1. SEM photomicrograph of Sample No. L13-10-53.



ORIGINAL PAGE IS
OF POOR QUALITY

Figure 2. SEM photomicrographs of Sample No. L13-P-36. (A) AFS (B) - (D) MFS.

A CRITICAL REVIEW OF THE SURFACE OXIDE LAYER ON Ti-(6Al-4V) ADHERENDS.

J. A. Skiles, J. Filbey, K. Sanderson and J. P. Wightman

ABSTRACT

Ti-(6Al-4V) oxide characterization, bond strength, and durability are the subjects of this literature review. Bond durability in various environmental conditions is discussed.

INTRODUCTION

Titanium and its alloys have excellent corrosion resistance, a high strength to weight ratio, and a high melting point (1812°C). Because of these characteristics and the abundance of ore, it is the material of choice for certain current engineering designs, such as high speed aircraft. Current engineering designs also rely upon structural adhesives. Consequently, it has become important to maximize titanium-adhesive bond strength and bond durability, in particular.

The strength and durability of an adhesive joint are influenced by many parameters. The choice of adhesive, the joint design and geometry, and induced loading stresses all affect bond strength. The adherend morphology and surface chemistry are also critical parameters. Current research is directed towards the production and characterization of a titanium oxide surface which maximizes bond strength. The influence of several factors upon the oxide which will affect bond durability such as aging, temperature, humidity and other environmental conditions, are also being investigated.

This paper is a review of current, published literature which describes:

1) Titanium-6% Aluminum-4% Vanadium (Ti-6Al-4V) oxides formed by

corrosion, chemical treatment, anodization, heating in vacuum and electron irradiation;

- 2) Ti-6Al-4V surface oxide chemistry and morphology after chemical pretreatment or anodization, and adhesion bond pull strength data and
- 3) preferred oxide morphology and structure to maximize bond strength and durability.

Titanium oxides can be amorphous and/or crystalline. If crystalline TiO_2 is formed, three structures are possible: anatase, brookite or rutile. Rutile has a greater entropy and a greater rate of formation than anatase⁽¹⁾.

Oxides Formed by Corrosion

Fraker and Ruff⁽²⁾ reported TiO_2 anatase formed on five titanium alloys exposed to a 3.5% NaCl solution at 100-200°C and pH = 6.8. Initially TiO and Ti_2O_3 formed and became TiO_2 at 150° - 200°C. The electron diffraction data supported the surface oxidation sequence⁽³⁾: $Ti + O \rightarrow Ti(O) \rightarrow Ti_6O \rightarrow Ti_3O \rightarrow Ti_2O \rightarrow TiO \rightarrow Ti_2O_3 \rightarrow Ti_3O_5 \rightarrow TiO_2$. Fraker and Ruff⁽⁴⁾ observed that increased saline solution acidity (with either HCl or H_2SO_4) increased the amount of TiO_2 anatase formed. Anatase did not form in corrosive saline solutions with NaOH. In a 12.5 pH solution, the diffraction pattern indicated the presence of $Na_2O \cdot 5 TiO_2$.

Koizumi and Nakayama⁽⁵⁾ reported that rutile TiO_2 is formed in a corrosive acid solution and was deposited on the surface.

Natan et al⁽⁶⁾ reported that anatase formed on titanium surfaces stripped of the natural oxide and then exposed to water for 24 hours at 95°C. Anatase was formed by a corrosion process and not by a surface oxide transformation. Furthermore, their data indicates that titanium can corrode in water at $\leq 100^\circ C$.

Oxides Formed By Vacuum Heating or Electron Irradiation.

The amorphous oxide can be transformed to small rutile crystals surrounded by larger anatase crystals (grain size $\sim 10\mu$) either by heating in vacuum (500°C 10^{-6} torr) or by electron irradiation ($10-100$ m Amperes/cm²).⁽⁷⁾ Since both treatments produced the same crystalline structure, the transformation was attributed to thermal effects, i.e., solid state crystallization.

Oxides Formed by Chemical Pretreatments and Anodization.

Ti-6Al-4V surface oxides produced by chemical pretreatments or anodization⁽⁸⁻¹⁷⁾ are described in Table I. The reported surface contaminants listed in Table I could be deleterious to titanium bond strength. Roche et al⁽¹⁴⁾ reported that non-titanium compounds of fluorine and water contaminants (i.e. NaF, CaF, KF,) may be formed on the Phosphate Fluoride (PF) etched surface. These compounds are easily hydrolyzed and can be removed by a water rinse in the PF process. As a result, the PF treated surface may have a nonhomogeneous surface topography. Chen et al.⁽¹⁸⁾ reported that approximately 0.2 of a fluorine monolayer chemisorbed on FPL etched aluminum resulted in adhesive/oxide interfacial failure. Fluorine atoms were weakly chemisorbed to the alumina rather than in the stable form of AlF_3 , as indicated by the decreased fluorine concentration with Auger measurements. There was a linear, inverse relationship between drum peel strength and fluorine surface concentration].

Ditchek et al.⁽¹³⁾ have reported that $\sim 65^\circ$ water rinses after a phosphate fluoride treatment removed KF and Na_3PO_4 contaminants. Otherwise, no other method to reduce pretreatment surface contaminants were noted in the literature.

Chemical Pretreatment and Anodized Ti-6 Al-4V Bond Strength and Durability Data

Table II is a compilation of bond strength and durability data for

chemically pretreated and anodized Ti-6 Al-4V. Two tests are commonly reported: wedge crack extension and tensile lap shear strength. It can be seen that bond strength and durability is affected by adhesion, temperature, relative humidity and the exposure time.

Ditchek et al(13,19) suggested that the bond strengths can be correlated with the surface oxide mechanical interlocking ability. The greater the degree of oxide micro-roughness ($< 0.1\mu\text{m}$), the greater the adhesive mechanical interlock, the higher bond strength and the greater durability. The pretreated surfaces were categorized into 3 groups according to micro-roughness, where Group I represents smooth oxide surfaces and Group III represents the most micro-rough surfaces (8). These categories are: Group I: PF, MPF; Group II: DA, TU, LP, DP; and Group III: CAA, AP. It is interesting to note that TU and LP treated adherends were similar in micro-roughness, yet only the TU treated adherend exhibited some interfacial failure in the wedge test results. Ditchek et al.(13) suggest that failure occurred along the Fe particles, which were present on both failed surfaces. These particles may represent stress risers which mechanically weakened the interface.

Hergenrother(20) reported that a 3 day water boil severely degraded the adhesive bond of a treated PF adherend. Whereas, the CAA with ammonium fluoride(21) maintained good bond strength. This is supportive of Ditchek's categorization of the surface oxides from pretreatment. The bond strength for the PF (Group I) adherend is primarily dependent upon Van der Waals forces, which were weakened by water. The CAA (Group III) adherend bond strength, with its high degree of micro-roughness, is primarily bonded through mechanical interlock.

Integral to bond durability is the oxide stability. Amorphous TiO_2 transformed to anatase TiO_2 under hydrothermal conditions may decrease bond strength(25). If the amorphous to crystalline transformation occurred in the

adhesive joint, the resulting stress could promote interfacial failure. To prevent this, the amorphous oxide could be precrystallized to anatase before bonding.(9) This would be advantageous since:

- 1) amorphous oxides have more oxygen vacancies than crystalline oxides(26). Oxygen diffusion from the interface, base metal corrosion, and structural oxide rearrangements are more likely for the amorphous oxide at elevated adhesive joint operational temperatures.
- 2) The Ti-O bond for the amorphous oxide is weaker than for the crystalline oxide as confirmed by AES sputtering(9).

Based upon Ditchek's et al.(13,19) data, the CAA oxide, precrystallized to anatase and free of contaminants, would be the optimum pretreatment for adhesive bonding.

Both water and elevated temperature(6) are important for the amorphous to crystalline anatase transformation. In vacuum, CAA oxide heated at $\leq 250^{\circ}\text{C}$ for one hour or 100°C for 24 hours did not transform.(6) As previously stated, treatment at 500°C in vacuum transformed the surface. However at 93°C in air, cubic TiO_3 , a possible anatase precursor, was formed(25). Ti-6Al-4V pretreated oxides (PF, MPF, DA, DP, LP, TU, CAA-5V or CAA-10V) did not undergo morphology changes when exposed to the following: 1) 79°C water immersion for 16 hours, or 2) 60°C 100% R.H. for 10 days.(19) However after 99°C water immersion for 210 hours, the initial amorphous oxide produced by PF, TU, CAA, or AP-9 was converted to TiO_2 anatase.(25) After water immersion for 24 hours at 95°C , anatase was evident on CAA(6). The CAA surface, which has a thick and porous oxide, more rapidly transformed to anatase.(25) This change was temperature dependent; it occurred after 4 hours water immersion at 140°C but did not occur after 400 hours at 60°C .(25) Although unexplained, the CAA oxide is more stable in salt water (3.5% wt NaCl) than pure water at $< 100^{\circ}\text{C}$ (9).

Given hydrothermal conditions at the oxide surface, oxide transformation mechanisms are suggested by Natan et al(6,9). Anatase nucleation from amorphous TiO_2 may be due to structural rearrangement, i.e. cubic TiO may be an anatase precursor. The anatase growth is attributed to a dissolution-precipitation mechanism in water.

Contaminant diffusion to the substrate may result in base metal corrosion and represents another mechanism for oxide transformation(6). The oxide transformation rate is increased by localized acidity(27). For example, increased acidity due to fluorine contaminants(27) may cause the TiO_2 oxide to corrode. Both increased oxide porosity and fluorine concentration have increased oxide transformation rates.(9) The porous CAA oxide transformed more rapidly than the nonporous oxides and even the porous, AP oxide, i.e., $CAA > PAA > TU > AP$. While CAA and AP oxides are both porous the CAA higher oxide transformation rate was attributed to the presence of fluorine on CAA (AP is fluorine free).

Iron contaminants in the pretreated oxide may influence the rate of oxide transformation from amorphous to rutile.(28) Conversely incomplete oxide transformation has been observed on TU, and attributed to iron contamination. The iron (calcium and magnesium, too) was deposited on the Ti-6A-4V surface after hot tap water rinses(29).

It should be noted that these hydrothermal, oxide transformations were reported for the pretreated, unbonded Ti-6A-4V surface. The mechanism is unknown which describes how water could penetrate the bondline and cause an interfacial oxide transformation at high humidity, and when the adhesive joint was exposed to high temperatures (260-315°C). Data suggest that water is transported along the bondline interface rather than through the adhesive(29).

CONCLUSIONS

Current reported literature indicate that the chromic acid anodization of titanium alloy Ti-6Al-4V produced optimum bond strength and durability. It has been suggested that precrystallization of the amorphous CAA oxide prior to bonding, without changing its morphology, may maximize oxide properties for bonding.

REFERENCES

- (1) F. Rossini, P. Cowie, F. Ellison and C. Browne. Properties of Titanium Compounds and Related Substances, Office of Naval Research, Dept. of Navy, Washington, D.C., 1956, pp. 84, 118.
- (2) A. C. Fraker and A. W. Ruff, Corrosion Sci., 11, (1971), 763.
- (3) I. I. Kornilov, Doklady Akad. Nauk. S.S.R., 183(5), (1968), 1087.
- (4) Anna C. Fraker and A. W. Ruff. Titanium Science and Technology Vol 4, ed. R. I. Jaffee and H. M. Burte, Plenum Press, N.Y.-London, 1973, pp. 2655.
- (5) T. Koizumi and T. Nakayama, Corrosion Sci., 8, (1968), 195.
- (6) Menachem Natan and John D. Venables, MML TR 82-20c, Martin Marietta Laboratories, MD. Prepared for Dept. of the Navy, September 1982.
- (7) Makoto Shiojiri, Journal of the Physical Society of Japan, 21, (2). (1966), 335.
- (8) B. M. Ditchek, K. R. Breen, T. S. Sun, and J. D. Venables, 25th Nat. SAMPE Symposium and Exhibition, Azusa, California (1980) 13.
- (9) Menachem Natan, Kathleen R. Breen and John D. Venables, MML TR 81-42(c), Martin Marietta Laboratories, MD. Prepared for Dept. of Navy, September 1981.
- (10) G. W. Lively, Technical Report AFML-TR-270, Jan. 1974.
- (11) K. W. Allen, H. S. Alsalim and W. C. Wake, J. Adhesion 6, (1974), 153.
- (12) K. W. Allen and H. S. Alsalim, J. Adhesion 6, (1974), 119.
- (13) B. M. Ditchek, K. R. Breen and J. D. Venables, MML TR-80-17-C. Martin Marietta Laboratories, MD. Prepared for Naval Air Systems Command, April 1980.

- (14) A. A. Roche, J. S. Solomon and W. L. Baun, *Appl. Surf. Sci.* 7, (1981), 83.
- (15) J. M. Abd El Kader, F. M. Abd El Wahad, H. A. El Shayeb and M. G. A. Khedr, *Br. Corrosion J.* 16, (2) (1981), 111.
- (16) John G. Mason, Ranjani Siriwardane and James P. Wightman, *J. Adhesion*, 11, (1981), 315.
- (17) Wen Chen, Ranjani Siriwardane and J. P. Wightman, 12th Nat. SAMPE Technical Conference (1980) 896.
- (18) J. M. Chen, T. S. Sun and J. D. Venables, 22nd National SAMPE Symposium and Exhibition, San Diego, California, April (1977) 25.
- (19) B. M. Ditchek, K. R. Breen, T. S. Sun and J. D. Venables, 12th National SAMPE Technical Conference (1980) 882.
- (20) P. M. Hergenrother and D. J. Progar, 22nd National SAMPE Symposium and Exhibition, San Diego, California (1977) 211.
- (21) Y. Moji and J. A. Marceau: U. S. Patent 3,959,091, May 25, 1976, The Boeing Co.
- (22) Roy D. Paul and Henry C. Winiarski, 22nd National SAMPE Symposium and Exhibition, San Diego, California (1977) 195.
- (23) S. Dias and J. P. Wightman, Submitted to L. H. Lee, Chairman of Symposium on Recent Developments in Adhesive Chemistry, Plenum Press, N.Y. (1984).
- (24) S. G. Hill, P. D. Peters and C. L. Hendricks, NASA Contractor Report 165944 Boeing Aerospace Company, Seattle, Washington 98124, July, 1982.
- (25) M. Natan, J. D. Venables and K. R. Breen, 17th National SAMPE Symposium (1982) 178.
- (26) J. W. Schultze, U. Stimming and J. Weise, *Ber. Bunsenges, Phys. Chem.* 86, (1982), 276.
- (27) F. Izumi and Y. Fujiki, *Bull. Chem. Soc. Japan*, 51, (6), (1978), 1771.
- (28) F. Izumi and Y. Fujiki, *Bull. Chem. Soc. Japan*, 69, (3), (1976), 709.
- (29) W. L. Baun, *J. Adhesion*, 12, (1981), 81.

TABLE I. A Description of Ti-6Al-4V Oxides Produced By Chemical Pretreatments or Anodization

<u>Method</u>	<u>Oxide Thickness (Å)</u>	<u>Surface Contaminants</u>	<u>Oxide Structure, Morphology and Chemistry</u>	<u>References</u>
1. Phosphate Fluoride (PF)	200	F Ca, P,N	1. relatively smooth surface, amorphous TiO ₂	(8,9)
				(17)
			2. cubic TiO	(9)
			3. TiO ₂ anatase	(10)
			4. TiO ₂ rutile	(12)
			5. pH 5.4-7.3	(16)
			6. surface enriched B phase (vanadium enriched and bcc)	(11)
		Na ₂ TiF ₆	7. TiO ₂ + TiF ₄	(14)
2. Modified Phosphate Fluoride (MPF)	80	F, Na	1. relatively smooth surface	(8,9)
3. Phosphate Fluoride-3 (PF-3)	NR	F, Cu	1. relatively smooth surface	(9)
4. VAST (VA-7)	NR	Si, Al	1. relatively smooth surface	(9)
			2. TiO ₂ anatase	(10)
5. Dry hone/PASA JELL 107 (DP)	100-200	Al ₂ O ₃ , F	1. macro-rough (protrusions > 1μm)	(8)
			2. TiO ₂ rutile + TiO ₂ amorphous	(10)
macro-rough: protrusions ≥ 1 μm		micro-rough: protrusions ≤ 1μm	NR: not reported	

Table I (Continued)

<u>Method</u>	<u>Thickness (Å)</u>	<u>Surface Contaminants</u>	<u>Oxide Structure, Morphology and Chemistry</u>	<u>References</u>
6. Liquid hone/PASA JELL 107 (LP)	200	Al ₂ O ₃ , F, Cr,	1. macro-rough	(8)
		N		(17)
7. Dapcotreat (DA)	60	Cr	1. macro-rough	(8)
8. Turco 5578 (TU)	175	Fe	1. macro-rough	(8,9)
			2. amorphous TiO ₂	(8,9)
		N, Na, Al		(17)
			3. cubic TiO	(9)
			4. rutile TiO ₂	(10)
			5. crystalline TiO ₂	(13)
6. ph of 7.3-9.2	(16)			
9. Chromic Acid Anodize (CAA)	5V - 400	F	1. micro-rough with ~10% of surface smooth porous oxide	(8,9,13)
	10V - 800			
		6% of F monolayer on surface	3. rutile TiO ₂	(13)
		P, N	4. TiO ₂ + Ti ₂ O ₃	(15)
			(17)	

macro-rough: protrusions $\geq 1 \mu\text{m}$ micro-rough: protrusions $< 1 \mu\text{m}$ NR: not reported

Table I (Continued)

<u>Method</u>	<u>Thickness (Å)</u>	<u>Surface Contaminants</u>	<u>Oxide Structure, Morphology and Chemistry</u>	<u>References</u>
10. Alkaline Peroxide (AP)	450-1350 depending upon process	Free of contamination some Na Ca, Al, N	1. micro-rough, porous oxide amorphous TiO ₂ 2. cubic TiO 3. rutile TiO ₂ 4. surface enriched B phase	(8,9,13,17) (17) (11,12,13) (17)
11. Hydrofluoric Acid, 4% w/v at 23°C	NR	NR	1. TiO ₂ rutile	(12)
12. Hydrochloric Acid, 10% w/v at 103°C	NR	NR	1. TiO ₂ rutile	(12)
13. Sulphuric Acid, 10% w/v at 103°C	NR	NR	1. TiO ₂ rutile	(12)
14. Anodization in 0.1 N sulphuric acid for 30 sec at 10-55 volts	NR	NR	1. TiO ₂ rutile	(12)

macro-rough: protrusions $\geq 1 \mu\text{m}$ micro-rough: protrusions $\leq 1 \mu\text{m}$

NR: not reported

TABLE II. Adhesive Bonding Results for Pretreated T1-6A1-4V Adherends.

<u>Test</u>	<u>Adhesive</u>	<u>Adherend Pretreatment</u>	<u>Crack Extension Results</u>	<u>Failure Analysis</u>	<u>References</u>
Crack Extension Test measured crack extension (inches) vs time (hrs) at 60°C 100% R.H.	FM 300K/BR127 adhesive/primer system	PF	1.4"/~750 hrs	adhesive failure primer lifted off adherend no Ti on primer	(13,19)
		MPF	2.0"/~750 hrs	adhesive failure primer lifted off adherend no Ti on primer	
		DA	0.4"/~750 hrs	less adhesive failure than for PF and MPF Ti on primer	
		DP	0.4"/~ 700 hrs	less adhesive failure than for PF and MPF No Ti on primer	
		TU	0.2"/~700 hrs	95% cohesive failure 5% adhesive failure primer on metal surface Fe on both sides of failed surface	
		LP	0.3"/~700 hrs	cohesive failure	
		CAA - 5V	~0.1"/680 hrs	cohesive failure	
		CAA - 10V	~0.1"/680 hrs	cohesive failure	

Table II (Continued)

<u>Test</u>	<u>Adhesive</u>	<u>Adherend Pretreatment</u>	<u>Pull Strength Results</u>	<u>Failure Analysis</u>	<u>References</u>
Tensile Lap Shear 60°C 100% RH	EA 9628H/BR 127 adhesive/primer	MPF	debonded after 61.2 hours at 800 psi	adhesive failure 100% R.H. did affect the surface morphology; anatase crystals formed	(13)
		LP	debonded after 1372 hours at 2000 psi.	adhesive failure 100% R.H. did not affect the surface morphology; similar to prebonded surface.	(13)
Tensile Lap Shear	~5 mil thick Polyphenylquinoxaline (PPQ)	PF	n=4 RT(4400 psi)	adhesive failure	(20)
			288°C (2500 psi)	adhesive failure	
			288°C after 300 hr aging 288°C (2400 psi)	adhesive failure	
			316°C (300 psi)	thermoplastic failure (PPQ TG is 318°C)	

1. n is number of test samples
2. RT is room temperature.

Table II Continued

<u>Test</u>	<u>Adhesive</u>	<u>Adherend Pretreatment</u>	<u>Pull Strength Results</u>	<u>Failure Analysis</u>	<u>References</u>
Tensile Lap Shear	~5 mil thick Polyphenylquinoxaline (PPQ)	PF	n = 4 Samples are boiled in H ₂ O 3 days. RT (<1000 psi)	100% adhesive failure	(20)
		CAA doped with Ammonium Fluoride	n = 4 RT(3530 psi) 288°C (730 psi)	20% adhesive failure thermoplastic failure	(20,21)

1. n is the number of test samples
2. RT is room temperature

Table II (Continued)

<u>Test</u>	<u>Adhesive</u>	<u>Adherend Pretreatment</u>	<u>Pull Strength Results</u>	<u>Failure Analysis</u>	<u>References</u>
Tensile Lap Shear	NR150 AG polyimide TG: 281-293°C	Adherend underwent the following: a. MEK degrease b. TURCO etch at 66° 15 min c. Water rinse (60°C) d. Distilled water rinse at RT e. Dry with nitrogen f. Sandblast 80 grit sand 60 PSI g. Dry with nitrogen h. Brush with Pasa Jell paste 107 i. Repeat (c)-(e)	n = 4 RT(3518 ± 179 psi)	NR	(22)
			177°C(3599 ± 561 psi)	NR	
			n = 3 177°C for 500 hours (2906 ± 467 psi)	NR	
			177°C for 1000 hours (3254 ± 255 psi)	NR	
			260°C for 500 hours (2660 ± 461 psi)	NR	
			260°C for 1000 hours (2889 ± 395 psi)	NR	
		n = 2 260°C (2292 ± 312 psi)	NR		

1. n is the number of test samples
2. RT is room temperature
3. NR is not reported.

Table II (Continued)

<u>Test</u>	<u>Adhesive</u>	<u>Adherend Pretreatment</u>	<u>Pull Strength Results</u>	<u>Failure Analysis</u>	<u>References</u>
Tensile Lap Shear	FM-34 Polyimide	Adherend underwent the following: a. MEK degrease b. TURCO etch at 66° 15 min c. Water rinse (60°C) d. Distilled water rinse at RT e. Dry with nitrogen f. Sandblast 80 grit sand 60 PSI g. Dry with nitrogen h. Brush with Pasa Jell paste 107 i. Repeat (c)-(e)	n = 16 RT(3081 ± 138 psi)	95% cohesive	(22)
			n = 12 316°C(1675±85 psi)	100% cohesive failure	
Tensile Lap Shear	L-13 polyimide	CAA 10V	232°C for 5000 hrs (1180 psi)	interfacial	(23)
			232°C for 500 hrs (2280 psi)	cohesive	
			232°C for 10,000 hrs (300 psi)	interfacial	
			49°C for 500 hrs (3000 psi)	cohesive	

Table II (Continued)

<u>Test</u>	<u>Adhesive</u>	<u>Adherend Pretreatment</u>	<u>Pull Strength Results</u>	<u>Failure Analysis</u>	<u>References</u>
Tensile Lap Shear	PPQ	CAA 10V	232°C for 10,000 hours (910 psi)	interfacial	(23)
			232°C for 500 hours (2560 psi)	cohesive	
			49°C for 500 hours (2850 psi)	cohesive	
Tensile Lap Shear	Redux BSL-308 (epoxy adhesive with aluminum powder filler and carbon black)	AP(0.24M hydrogen peroxide for ~ 7 hours)	10,694 psi	cohesive	(11)
		4% w/v HF solution ~ 2 min.	8,526 psi	cohesive	

Table II (Continued)

<u>Test</u>	<u>Adhesive</u>	<u>Adherend Pretreatment</u>	<u>Pull Strength Results</u>	<u>Failure Analysis</u>	<u>References</u>	
Tensile Lap Shear	NR056X		n = 5 PSI at RT/PSI at 232°C			
		1. CAA 10V ¹	4250/2740	NR	(24)	
		2. Phosphoric Acid Anodize ¹	3250/2350			
		3. LP	1030/1010			
		4. PF (Picatinny Method)	1660/2150			
		5. PF (Grit Blast)	1150/1160			
		6. PF (BAC 5514)	1140/1460			
		7. RAE Process (H ₂ O ₂ + NaOH)	1100/1630			
	8. TU	2730/1760				
	FM 34					
		1. CAA 10V ¹	3760/2320	(24)		
		2. Phosphoric Acid Anodize ¹	2960/2490			
		3. LP	2810/2150			
		4. PF (Picatinny Modified)	2910/2400			
		5. PF (Grit Blast)	2930/1840			
		6. PF (BAC 5514)	2970/2560			
7. RAE Process (H ₂ O ₂ + NaOH)		2850/2490				
8. TU	2780/2510					

¹Phosphoric acid anodize and Chromic acid anodize were both considered to be superior for all adhesives tested.

S. G. Hill et al⁽²⁴⁾ reported that CAA had good thermal stability; but PAA is not stable after 125 hrs exposure at 315°C.

NR is not reported. RT is room temperature.

Table II (Continued)

<u>Test</u>	<u>Adhesive</u>	<u>Adherend Pretreatment</u>	<u>Pull Strength Results</u>	<u>Failure Analysis</u>	<u>References</u>
			PSI at RT/PSI at 232°C n = 5		
Tensile Lap Shear	LARC-13	1. CAA 10V	2980/2200	cohesive failure for LARC-13 samples	(24)
		2. Phosphoric Acid Anodize	2490/2030		
		3. LP	850/560		
		4. PF (Picatinny Modified)	1610/1290		
		5. PF (Grit Blast)	1470/1180		
		6. PF (BAC 5514)	1650/1490		
		7. RAE Process (H ₂ O ₂ + NaOH)	2280/1910		
		8. TU	2120/1840		
PPQ		1. CAA 10V	5250/2820	cohesive failure for PPQ samples	(24)
		2. Phosphoric Acid Anodize	5400/3510		
		3. LP	1730/2220		
		4. PF (Picatinny Modified)	2360/2800		
		5. PF (Grit Blast)	1460/2460		
		6. PF (BAC 5514)	1950/2420		
		7. RAE Process (H ₂ O ₂ + NaOH)	2690/2768		
		8. TU	3130/2830		

Table II (Continued)

<u>Test</u>	<u>Adhesive</u>	<u>Adherend Pretreatment</u>	<u>Crack Extension Results</u>	<u>Failure Analysis</u>	<u>References</u>
Crack Extension Test measured crack extension (inches) after 10,000 hrs	LARC-13	CAA-10V	0.37"/2.12"	2.12" Failed	(24)
		PASA JELL 107	0.71"/1.55"	1.55" Failed	
	PPQ	CAA-10V	0.44"/1.68"	1.68" Failed	
		CAA-5V	0.34"/2.20"	2.20" Failed	
	NR056X	CAA-10V	0.80"/0.24"	No Reported Failure	
		PASA JELL 107	0.54"/0.31"	No Reported Failure	

49° 100% RH/232°C
n = 5